

## CANADIAN THESES ON MICROFICHE

## THESES CANADIENNES SUR MICROFICHE



National Library of Canada  
Collections Development Branch

Canadian Theses on  
Microfiche Service

Ottawa, Canada  
K1A 0N4

Bibliothèque nationale du Canada  
Direction du développement des collections

Service des thèses canadiennes  
sur microfiche

### NOTICE

The quality of this microfiche is heavily dependent upon the quality of the original thesis submitted for microfilming. Every effort has been made to ensure the highest quality of reproduction possible.

If pages are missing, contact the university which granted the degree.

Some pages may have indistinct print especially if the original pages were typed with a poor typewriter ribbon or if the university sent us an inferior photocopy.

Previously copyrighted materials (journal articles, published tests, etc.) are not filmed.

Reproduction in full or in part of this film is governed by the Canadian Copyright Act, R.S.C. 1970, c. C-30. Please read the authorization forms which accompany this thesis.

### AVIS

La qualité de cette microfiche dépend grandement de la qualité de la thèse soumise au microfilmage. Nous avons tout fait pour assurer une qualité supérieure de reproduction.

S'il manque des pages, veuillez communiquer avec l'université qui a conféré le grade.

La qualité d'impression de certaines pages peut laisser à désirer, surtout si les pages originales ont été dactylographiées à l'aide d'un ruban usé ou si l'université nous a fait parvenir une photocopie de qualité inférieure.

Les documents qui font déjà l'objet d'un droit d'auteur (articles de revue, examens publiés, etc.) ne sont pas microfilmés.

La reproduction, même partielle, de ce microfilm est soumise à la Loi canadienne sur le droit d'auteur, SRC 1970, c. C-30. Veuillez prendre connaissance des formules d'autorisation qui accompagnent cette thèse.

**THIS DISSERTATION  
HAS BEEN MICROFILMED  
EXACTLY AS RECEIVED**

**LA THÈSE A ÉTÉ  
MICROFILMÉE TELLE QUE  
NOUS L'AVONS REÇUE**

**Canada**

**Contribution to the Field Measurement  
of Low Impedance  
Extended Grounding Systems**

**Hector G. Sarmiento-Uruchurtu**

**A Thesis  
in  
The Department  
of  
Electrical Engineering**

**Presented in Partial Fulfillment of the Requirements  
for the Degree of Doctor of Philosophy at  
Concordia University  
Montréal, Québec, Canada**

**May 1985**

**© Hector G. Sarmiento-Uruchurtu, 1985**

## ABSTRACT

### Contribution to the Field Measurement of Low Impedance Extended Grounding Systems

Hector G. Sarmiento-Uruchurtu, Ph.D.  
Concordia University, 1985

The purpose of this dissertation is to evaluate different field measurement techniques of ground impedances of electric power substations. Emphasis is placed to those cases where the ground impedance magnitude is below  $1.0 \Omega$ , and to analyze problems associated with these measurements, primarily the mutual coupling effects between auxiliary current and potential leads.

The investigation begins with a review of the two types of ground testing used: high current injection and low current injection. Following this, extensive experimental data is presented, collected from a series of grounding tests performed at two substations of Hydro-Quebec's power network. In particular, it is concluded that low current injection methods with magnitudes as low as 100 mA, can give results comparable to a more expensive and less safe high current method.

Also, as a result of numerous field measurements with

low current methods, the undesirable effect of mutual coupling between auxiliary test leads was experimentally verified and favorably compared to curves determined analytically. It is also shown how accurate results can be obtained, for any value of the angle between the auxiliary leads, provided the mutual effects are minimized by the use of proper analytical tools. Subsequently, a technique is presented by which the value of the ground impedance is determined, using interpolating and smoothing techniques applied to a curve of ground impedance magnitudes at different angles between the auxiliary leads.

The final part of this dissertation presents an extension to the work previously done in calculating the mutual impedance of grounded conductors of finite length lying on the surface of the ground. Equations are developed taking into account the fact that one of the conductors may be at any height above the earth's surface. This has particular applications in urban and suburban areas, where it is not always possible to lay cables on the ground. A sensitivity analysis is presented to show the influence of the different parameters involved.

## ACKNOWLEDGEMENTS

I am indebted to my wife Marilu for her patience, encouragement, and sacrifices throughout the completion of this research. I am also indebted to my parents, who have always stood behind me.

To my thesis supervisors, Dr. Dinkar Mukhedkar and Dr. V. Ramachandran, my total appreciation for their guidance throughout the course of this work.

This investigation could not have been possible without the facilities and close collaboration offered by Hydro-Quebec's Essais des Reseaux et Analyse, my thanks to J.R. Valotaire, Chef de Service, and Jean Claude Deslaurier, Chef de Division Reseaux, and specially to Jacques Fortin with whom I had many interesting and rewarding discussions for the last four years.

I am also grateful to the Instituto de Investigaciones Electricas and Consejo Nacional de Ciencia y Tecnologia for their financial assistance.

## TABLE OF CONTENTS

### 1. INTRODUCTION

- 1.1 General Background.....1
- 1.2 Scope of the Thesis.....3

### 2. BASICS OF GROUND IMPEDANCE MEASUREMENTS

- 2.1 Nature of the Problem.....7
- 2.2 Ground Impedance Measurements.....11
  - 2.2.1 Current Measurements.....14
  - 2.2.2 Potential Measurements.....14
- 2.3 Other Measurements in Grounding Systems
  - 2.3.1 Current Distribution.....15
  - 2.3.2 Touch and Step Voltages.....19

### 3. FIELD MEASUREMENT TECHNIQUES FOR SUBSTATION

#### GROUND IMPEDANCE. HIGH CURRENT INJECTION

- 3.1 General.....22
  - 3.1.1 Current Measurement.....23
  - 3.1.2 Potential Measurement.....23
  - 3.1.3 Shielding Factor.....24
- 3.2 Synchronous Power-Frequency Method.....25
- 3.3 Interference Compensation Method.....30
- 3.4 Beat-Frequency Method.....32
- 3.5 Frequency Different from Power-Frequency Method.....34
- 3.6 Safety During Field Measurements.....36

### 4. FIELD MEASUREMENT TECHNIQUES FOR SUBSTATION

#### GROUND IMPEDANCE. LOW CURRENT INJECTION

- 4.1 General.....39
- 4.2 Oscillator-Voltmeter Method.....41

4.3 Instrument for Ground Impedance Measurements.....	43
4.4 Frequency-Scanning Method.....	45
5.COMPARATIVE FIELD MEASUREMENTS WITH HIGH AND LOW CURRENT INJECTION METHODS	
5.1 Introduction.....	51
5.2 Resistivity Measurements.....	52
5.3 High Current Method and Results.....	55
5.4 Low Current Injection Method.....	58
5.4.1 Instrumentation.....	58
5.4.2 Measurement Points.....	60
5.4.3 Analysis of Field measurements.....	60
5.4.4 Final Results.....	63
5.5 Interpolation of the Final Ground Impedance Without Calculating Mutual Coupling Effects.....	66
6 .MUTUAL COUPLING EFFECTS BETWEEN AUXILIARY CURRENT AND POTENTIAL LEADS	
6.1 General Background.....	77
6.1.1 Mutual Impedance Between Two Conductors in the Scope of Low Ground Impedance Measurements.....	78
6.1.2 Two Conductors Lying on the Surface of the Ground.....	80
6.2 Analytical Development	
6.2.1 Basic Assumptions.....	83
6.2.2 Solution to the Neumann Integral.....	84
6.3 Sensitivity Analysis.....	97
7. CONCLUSIONS.....	103

8. REFERENCES.....	106
--------------------	-----

#### APPENDIX A

Instrumentation Required for Measuring Ground Impedance.....	113
---	-----

#### APPENDIX B

Theory of the Fall-of-Potential Method.....	121
---	-----

#### APPENDIX C

Screening Factor at Yamaska Substation.....	126
---	-----

#### APPENDIX D

Computation of the Test Current Magnitude in the Ground Impedance Measurements at Yamaska Substation....	129
---	-----



## LIST OF FIGURES

2.1 Fall-of-Potential Method.....	9
2.2 Plot of $R_g$ vs. distance $P$ to potential electrode...	9
2.3 Ground Fault current distribution in a power substation.....	15
2.4 Standard set-ups for measuring a) touch voltage and b) step voltage.....	21
3.1 General lay-out of the synchronous power-frequency method.....	27
3.2 Potential rise measurement with both polarities....	28
3.3 Phasor diagram of measured and residual voltages...	28
3.4 General lay-out of the interference compensation method.....	31
3.5 General lay-out of the beat-frequency method.....	33
3.6 Method for measuring test signals in presence of 50 Hz interference.....	38
4.1 Dependence of the product of ground impedance and screening factor upon increasing test voltage at three 110 kV substations [28].....	40
4.2 General lay-out for the oscillator-voltmeter method.....	42
4.3 Plot of $R_g$ (or $X_g$ ) against frequency.....	46
4.4 Plot of ground impedance vs. distance $P$ at Tesistan substation.....	47
4.5 General lay-out of the frequency-scanning method...	50
5.1 Hydro-Quebec's Yamaska Substation.....	53

5.2 Short-circuit testing set-up.....	54
5.3 Potential probe locations for	
High Current injection.....	57
5.4 Ground impedance profile in High Current Testing....	57
5.5 Low Current injection circuit.....	59
5.5 Upper curve: Transfer impedance phase angle	
Lower curve: Transfer impedance magnitude.....	62
5.7 Probe directions in the frequency-scanning method..	62
5.8 Ground impedance vs. distance P for direction $P_5$ ..	64
5.9 Ground impedance vs. distance P for direction $P_1$ ..	64
5.10 Ground impedance at different angles	
between P and C auxiliary leads.....	67
5.11 Analytically determined mutual reactance ( $X_{SS}$ )	
against angle between P and C (from Ref. [45])...	68
5.12 Ground Impedance vs. angle $\theta$ after applying	
smoothing subroutine.....	71
5.13 Delta-star 120-25 kV three-phase transformer.....	72
5.14 Truck inside Becancour substation where all	
field measurements were procured.....	73
5.15 Test bench: Where all signals from current and	
potential probes are collected.....	74
5.15 Spectrum analyzer, filter, and oscillator,	
utilized in the Low Current injection methods.....	75
5.17 Ammeter and power source for the Low Current	
injection methods.....	76
6.1 Conductor arrangement for mutual impedance	

calculation.- Parallel directions.....	85
6.2 Conductor arrangement for mutual impedance	
calculation.- Angle between their directions.....	85
6.3 Effect of the resistivity and height	
on the mutual impedance.....	100
6.4 Effect of the height and distance between	
conductors on the mutual impedance.....	101
6.5 Effect of the angle between conductors on	
the mutual impedance.....	102
B.1 Fall-of-Potential Method.....	121
C.1 Single circuit 120 kV line at Yamaska.....	126
C.2 Screening factor calculation.....	128
D.1 Typical output from oscillographic recorder.....	129

## LIST OF SYMBOLS

$C$  = Auxiliary current electrode, also distance to current electrode in m.

$P$  = Auxiliary potential electrode, also distance to potential electrode in m.

$P_i$  = Potential electrode directions for low current testing ( $i=1,2,\dots,5$ )

$M$  = General expression for the Neumann integral.

$y$  = Horizontal distance between conductors, in m.

$z$  = Height of one conductor, in m.

$r$  = Screening or shielding factor.

$I_m$  = Measured test current magnitude in amperes.

$I_i$  = Initial current in the de-energized test circuit in amperes.

$I_{ma}$  = Current measurement in the synchronous power-frequency method (position "a"), in amperes.

$I_{mb}$  = Current measurement in the synchronous power-frequency method (position "b"), in amperes.

$I_{max}$  = Current maxima measured because of the phase shift between the injected current and the residual current in the beat-frequency method, in amperes.

$I_{min}$  = Current minima measured because of the phase shift between injected current and the residual current in the beat-frequency method, in amperes.

$I_{in}$  = Induced current in the overhead ground wires due to

current circulating in the phase conductors, in amperes.  $= (1-r)I_{fl}$

$I(V_m)$  = Current responsible for the voltage rise  $= I_m - I_{in}$ , in amperes.

$I_f$  = Earth-fault current, in amperes.

$I_{ft}$  = Magnitude of ground fault current returning through the transformer neutral, in amperes.

$I_{fl}$  = Magnitude of ground fault current supplied by h.v. transmission line  $= I_m$ , in amperes.

$I_g$  = Magnitude of ground fault current into the earth  $= r I_{fl}$ , in amperes.

$I_s$  = The part of  $I_{fl}$  circulating through overhead ground wires and tower footings, in amperes.

$I_t$  = Conductive current that flows through the overhead ground wires and tower footings, in amperes.

$I_{gg}$  = Part of  $I_g$  flowing into the ground grid.

$Z$  = Measured value of substation ground impedance in ohms  
 $= R + jX$

$Z_m$  = Calculated mutual ground impedance between the auxiliary probes in ohms.

$Z_g$  =  $Z - Z_m$  = Substation ground impedance in ohms.  
 $= R_g + j X_g$

$Z_{mw}$  = Mutual impedance between overhead ground wires and phase conductors in ohms.

$Z_{sw}$  = Self-impedance of overhead ground wires with earth return in ohms.

GPR = Ground Potential Rise of the substation earthing

system in the event of any type of ground fault (in volts).

$V_m$  = Measured potential rise due to the test current, with respect to remote earth (in volts).

$V_i$  = Initial voltage in the de-energized test circuit (in volts).

$V_{ma}$  = Potential measurement in the synchronous power-frequency method (position "a"), in volts.

$V_{mb}$  = Potential measurement in the synchronous power-frequency method (position "b"), in volts.

$V_{max}$  = Potential maxima measured because of the phase shift between the potential rise due to the test current in the beat-frequency method and the residual voltage, in volts.

$V_{min}$  = Potential minima measured because of the phase shift between the potential rise due to the test current in the beat-frequency method and the residual voltage, in volts.

$V_c$  = In the interference compensation method, the voltage produced to compensate the residual voltage, in volts.

$\omega$  = Angular frequency, in rad/s

$\gamma$  = Propagation constant for plane electromagnetic waves.

$\mu$  = Permeability of the medium, in H/m

$\rho$  = soil resistivity in ohm-m.

$\theta$  = Angle between P and C in degrees.

$\phi$  = Substation ground impedance phase angle in degrees.

- Ⓞ = Oscillator, power source.
- Ⓥ = Voltmeter (frequency selective, when needed).
- Ⓐ = Current meter
- Ⓛ = filter

## CHAPTER 1

### INTRODUCTION

#### 1.1 General Background.

The first use of the earth as a return conductor was announced by Steinheil in the "Comptes Rendus" of September 10, 1832 for electric telegraphic communications. Although at that time, the earth was viewed as a reservoir presenting no resistance to the return current and introducing no interference between parallel returns.

In the area of electric power engineering, for the last hundred years or so, grounding systems have played an important role. The earth is commonly and frequently used as an electrical conductor for systems returns because its resistance can be quite low owing to the large cross-sectional area of the electrical path, although its resistivity is high compared to that of a metallic conductor.

Some decades ago, many people believed that any grounded object, however crudely, could be safely touched. Nowadays, basic problems involving the earth, as well as buried conductors and/or grounded aerial conductors, necessitate theoretical solutions that are more complex than



that of metallic circuits only [23], first of all, because the great extent of the earth calls for the use of electromagnetic field theory rather than conventional transmission line and circuit theory in the solution of most of the problems. Other factors that may complicate the analysis are, for example, ionization effects due to high voltages or to electrolytic action, and the heterogeneous character of the earth.

One area of earth conduction effects that receives much attention these days is the analysis and design of electric power substation grounding systems. As demand for electricity grows, and short circuit levels in modern power systems increase, so does the number and complexity of power substations, reflecting an important need for accurate design procedures for grounding systems, both from a safety point of view and from financial considerations [7,23,38].

Basically, a safe grounding system has two objectives:

- 1).-Provide means to carry and dissipate electric currents into ground under normal and fault conditions, without exceeding any operating and equipment limits or adversely affecting continuity of service.
- 2).- Assure such a degree of human safety that a person working or walking in the vicinity of grounded facilities, who may come near an electrically conductive object tied to

the grounding system under the influence of a major ground fault, is not exposed to the danger of a critical electric shock.

With the above in mind, the design then must minimize the ground potential rise (GPR) of the grounding system in the event of a ground fault. The objective is to limit the interference over control and communication cables, and to limit the potentials transferred via services connected to the substation such as telephones, water supplies, etc. But most important of all, the purpose is to keep potential gradients at the surface of the earth down to a safe level, both outside the boundary to protect the public, and inside the substation to protect personnel who may also be endangered by either touch or step potentials [37,23,24].

The assessment of the possible dangerous conditions just mentioned demands a reasonably high degree of accuracy in the value of the substation ground impedance; since this parameter, along with the magnitude of the fault current circulating into the ground, determines the magnitude of the GPR.

## 1.2 Scope of the Thesis.

The substation ground impedance can be determined analytically or experimentally, and in general, a grounding

system may be analyzed, using several methods, including:

- 1) Approximate formulas.
- 2) Analytical methods.
- 3) Graphic techniques.
- 4) Measurements from scale models.
- 5) Field testing of actual substations.

The present thesis addresses this last area. Field measurement techniques, when properly executed, will provide a reliable value of the substation ground impedance, and are particularly important when verifying the adequacy of an existing substation, in the case where many additions have been made over the years and the original design is obsolete.

Recently, the technical literature has reported some new methodologies for measuring ground impedances when there is a significant inductive component in the grounding system, and interest in the accuracy of all of them has increased lately [36,41]. Chapter 2 discusses some of the fundamentals common to ground testing, and states the importance of measuring the reactive part of the ground impedance. It also discusses some of the advantages and disadvantages of both high current (HC) and low current (LC) injection techniques. Chapters 3 and 4 review these HC and LC methods, pointing out specific characteristics of each

one of them.

Field testing is normally done either by using high levels of injected current, e.g. staged-fault tests, or low levels of injected current, e.g. using a portable earth tester. A comparison of the different techniques seemed to be the next logical step. In this investigation, Chapter 5 presents results from two Hydro-Quebec's power substations, comparing the frequency-scanning low current method with a high current injection technique, as first reported in reference [40], and it is concluded that both methods give comparable results.

On the other hand, low current (LC) methods have the disadvantage of mutual coupling effects between the auxiliary leads. Reference [45] presents a technique for calculating these effects between any two wires lying on the surface of the earth, and accounting for such parameters as soil resistivity, frequency, length of potential and current leads (so called "end effects"), and the angle between them. These equations had not been substantiated with enough field data. In the measurements reported here, though, using an LC method, the effect of mutual coupling is clearly seen. A successful application of this technique is achieved, thus reinforcing the convenience of low current methods. This problem of mutual effects between the auxiliary test wires is taken one step further in this work, in two different ways:

First, smoothing and interpolating techniques are applied to a curve of ground impedance vs. angle between auxiliary leads. With these techniques, the ground impedance magnitude at 90 degrees is extracted (where mutual coupling is minimum). This is useful whenever measurements are not possible with the test leads perpendicular to each other, but measurements at other angles are available. This simple technique was verified by comparing it with results from a high current test.

Second, an extension to the work done for two conductors lying on the earth's surface is presented in Chapter 5, generalizing the expressions for mutual impedance by allowing one of the conductors to be at any height, including resting on the soil's surface (zero height).

In summary, the present work was carried out with the purpose of making a contribution to the field testing of low ground impedances.

## CHAPTER 2

### BASICS OF GROUND IMPEDANCE MEASUREMENTS

#### 2.1 Nature of the Problem.

When speaking of ground resistance or impedance field measurements, the principle is the same, current should be injected through the earth, and the only way to do this is by inserting electrodes into the soil. Much of the fundamental work for ground testing was done at the National Bureau of Standards in the period 1910-1920, and portable instruments for resistance measurements became available around 1927. It is interesting to note that at this time some books on electrical measurements [30] do not even mention the subject.

Until recently, field testing of an electric power substation consisted of measuring only the resistance to remote ground (neglecting the reactive component) with a commercial earth tester, and the methods prescribed in the literature required that the resistance of the substation ground grid be determined with all electrical conducting paths disconnected from the grid [21]. These "alternative paths" consist of overhead ground wires, distribution neutrals, counterpoises, communication cable shields, and any other metallic conductor connected to the grid.

Although other techniques for measuring the resistance of an earth electrode exist [45], the most common method for determining the substation ground grid resistance is the one known as the fall-of-potential method, illustrated in figure 2.1. and explained in Appendix B.  $R_g$  is the ground grid resistance to be measured and P and C are respectively, a potential and a current auxiliary electrode, placed at suitable distances from the substation and parallel to each other. A known current ( $I_m$ ) is passed between the grid and electrode C, measuring at the same time the potential ( $V_m$ ) between the grid and auxiliary electrode P. So the ratio  $V_m/I_m$  gives the resistance  $R_g$ . The reason modern earth testers used in this application give only the value of the dc resistance is that they produce a reversing dc in the form of a square wave, with a zero period at each polarity reversal, to avoid possible polarization effects. Reference [25] provides a good historical discussion on some models commercially available.

A unique characteristic of an earth electrode is that its resistance is practically determined by the body of earth surrounding the electrode. So in the above method it is very important that the resistance areas of  $R_g$ , C and P do not overlap. This is achieved by plotting the values of  $R_g$  against the distance of P to the substation ground grid as shown in figure 2.2. If the current electrode C is at a distance  $d_1$  (resistance areas overlapping), a series of

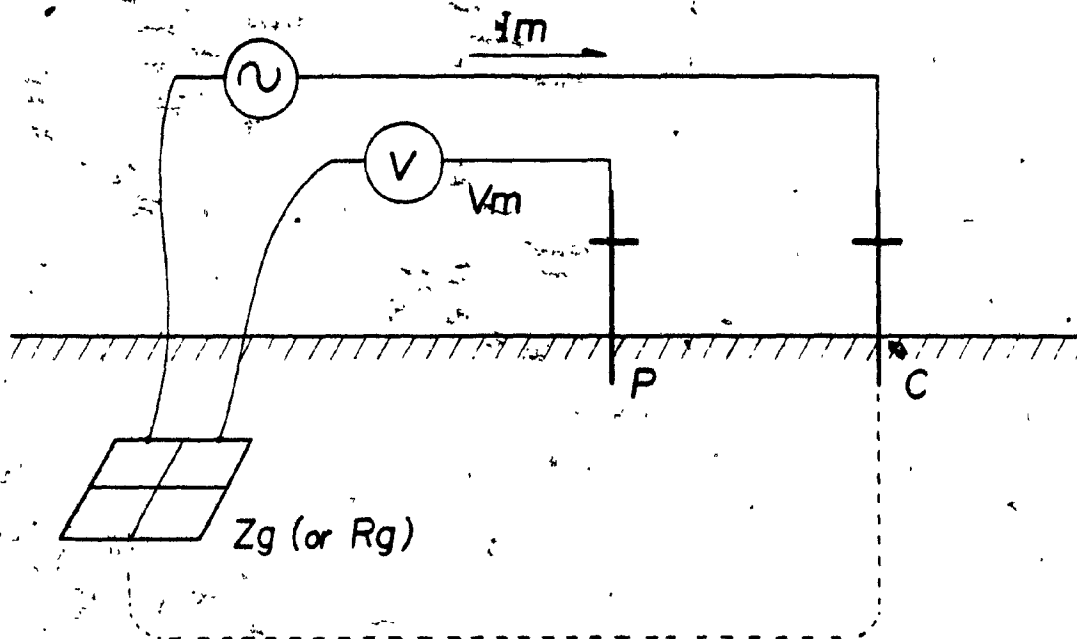


FIGURE 2.1

Fall-of-Potential Method

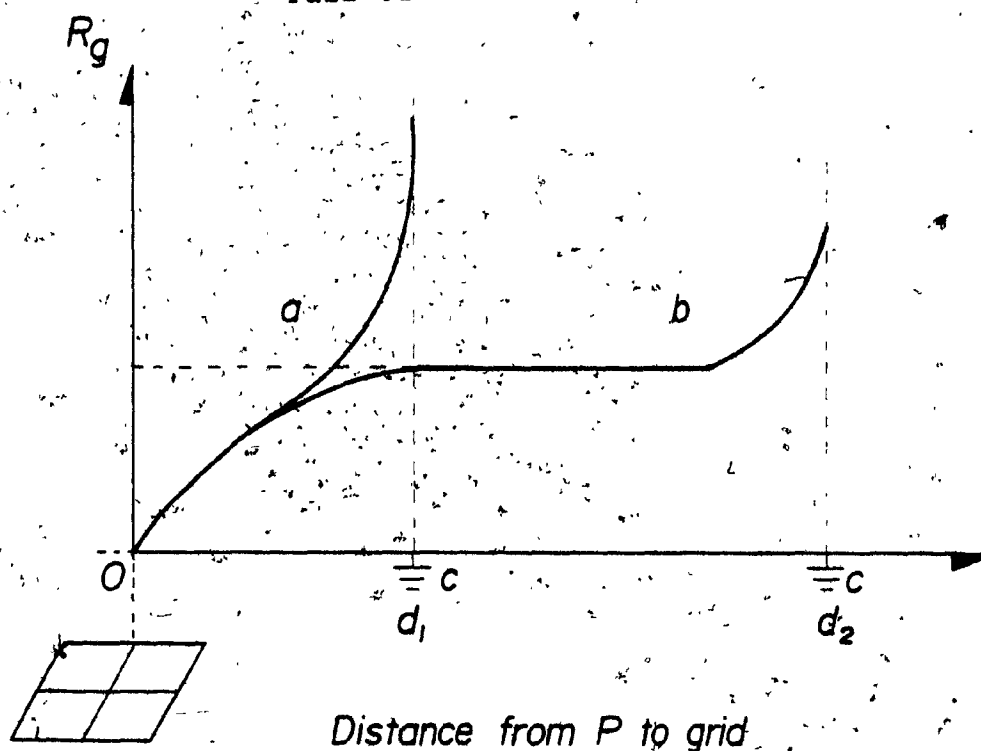


FIGURE 2.2

Plot of  $R_g$  vs. distance  $P$   
to potential electrode.



measurements made with the potential electrode P at various distances from the substation will result in curve "a". The measured resistance is increasing steadily as P is moved along the line joining the earth electrode and C. On the other hand, if C is moved to a distance  $d_2$  such that the resistance areas do not overlap, a curve of the type "b" will result. The resistance corresponding to the flat (horizontal) section is the true value of the resistance of the ground grid. If the area covered by the ground grid is so large that a suitable distance for C cannot be found, an extension to the fall-of-potential method called the "slope method" [44] can be applied.

Theoretically, in the fall-of-potential method, the ground resistances of the P and C electrodes do not influence the measurement, since they are taken into consideration by the method itself [24]. Nevertheless, in practice, these resistances should not exceed a maximum value beyond which the test current is either lower than the instrument's sensitivity or similar to the stray currents in the earth. To avoid one or both of the conditions above, the test current is increased by lowering the auxiliary electrode resistance. This is done by driving the rod deeper into the soil, pouring water around the rod, and/or driving additional ones, interconnecting them together.

Many years ago it was recognized that the measurement

of grounding electrodes might have a significant reactive component [21,11], but until recently it is becoming more and more accepted that these extended ground conductors ("alternative paths", as we have called them before) introduce a significant reactive component that could increase the value of the GPR if only the resistance component is measured (since these alternative paths will also drain current in the event of a ground fault), and consequently must be included in the measurement. This latter fact was first recognized in reference [29]. A high inductive component in the substation ground impedance may cause a substantial error when calculating the GPR using only the value of  $R_g$ . For example: If the calculated fault current into the grounding system is 4900 A, and the measured resistance is one ohm, then the GPR = 4900 V, but if an inductive component is present (say,  $Z_g = 1.12 \Omega$ ), then the GPR is actually 5488 V. This value might be too high by some standards [4]. A practical example is given in [1] where tests performed on a de-energized 400 kV substation, showed a dc resistance 3% lower than the 50 Hz impedance.

## 2.2 Ground Impedance Measurements.

In general, for all electric power substations (but particularly for EHV substations) whose grounding systems comprise extended conductors ("alternative paths") connected

to the main grid, its impedance may include a significant reactive component, and measurements cannot be made with traditional low voltage portable earth testers.

As stated previously, in order to determine the impedance of a substation grounding system, a known current ( $I_m$ ) must be circulated between this impedance ( $Z_g$ ) and a remote current electrode (C) via an auxiliary wire, measuring at the same time the voltage rise ( $V_m$ ) of the grounding system relative to an auxiliary potential reference electrode (P) at "remote ground". By remote ground it is meant that the potential probe must be at a zero reference point (ideally) to detect the full potential rise of the grounding system. To find the correct value of  $V_m$ , this auxiliary potential electrode is placed at increasing distances from the substation until the difference between at least two or three successive readings is negligible.

Hence, the evaluation of a substation ground impedance comprises, basically, two types of measurements: Current and potential. If it were possible to install an ideal remote ground reference point and if it were always possible to assure the complete isolation of the test and current return electrodes, ground impedance measurements would be a simple process. But since the ground impedance of any conductor is comprised mostly by the earth surrounding the electrode,

many difficulties need to be overcome. Generally speaking, measurement problems become more difficult as the dimensions of the grounding system increase, as the impedance of the grounding system decreases, and as the level of ambient noise and soil resistivity both increase. The measuring techniques that have been proposed lately are described in the next two chapters and are arbitrarily divided into high current (a minimum of 50 A as suggested in [28]), and low current (approximately < 10 A) injection techniques. The basic difference among all techniques (both LC and HC) lies mainly in the magnitude, frequency and source of the injected currents. All methods are geared to minimize the effects of residual voltages. These voltages have usually prominent harmonics and result from residual or stray system currents circulating through the ground impedance.

Although with high current testing techniques it is possible to determine the efficiency of each grounding element, by measuring the current distribution [15,15], LC testing has the following advantages over HC testing:

- 1) The man-hours required to complete the field measurements may be two or three times less, making them less expensive.
- 2) There is no partial use of the power system, whilst for HC testing a transmission line has to be made available, with the corresponding modifications in the protection coordination.
- 3) There is no need to account for the induced current in

the overhead ground wire(s).

4) And most important of all, it poses less danger to shock hazards.

#### 2.2.1 Current Measurements.

Another basic difference between HC and LC methods is that the former commonly uses a phase conductor of a transmission line for current injection, while the latter uses a temporary field cable or a telecommunication line. The most relevant requirement for measuring the current is that the auxiliary current probe (C) be located far away so that there is no overlapping in the impedance areas. As a rule of thumb, a distance of  $5D$  or  $10D$  is chosen [28], where  $D$  is the equivalent diameter of the area covered by the substation grounding system. Of course, for extended systems, knowing the equivalent diameter might prove impossible. In such a case,  $5D$  or  $10D$  should be used as a first approximation or starting point (with  $D$  the equivalent diameter of the ground grid only). If no zero slope is seen from the  $Z_g$  vs.  $P$  curve, then  $C$  should be placed farther away.

#### 2.2.2 Potential Measurements.

As mentioned before, the voltage rise ( $V_m$ ) of the substation under study must be measured with respect to a

remote reference point, which must be chosen using the following guidelines:

- a) Its distance to the substation must be large enough to be outside the zone of influence of the potential profile around the substation.
- b) The path between the remote ground and the substation should not come close to induction sources (i.e. transmission lines or distribution lines).
- c) There should be no metallic structures in the vicinity (i.e. underground pipes).

In order to validate the measured voltage rise, several distant locations around the substation may be used. To reach the potential probe (P), the common practice is to lay out temporary field cables, for example, multiconductor cables with four No. 22 copper conductors, two of which are normally used to check cable continuity.

### 2.3 Other Measurements in Grounding Systems.

#### 2.3.1 Current Distribution.

When a ground fault occurs inside an electric power substation, the total earth fault current  $I_f$  (that is, the current flowing into the equipment's ground conductor at the point of fault), is divided into two parts [33]: (refer to figure 2.3)

- 15 -

1) The part flowing in the ground grid and returning through the transformer neutral ( $I_{ft}$ ).

2) The portion of the ground fault current supplied by the HV transmission line ( $I_{fl}$ ).

That is:

$$I_f = I_{ft} + I_{fl} \quad (2.1)$$

$I_{fl}$  itself is divided into the part  $I_{gg}$  going into the ground grid and returning through the earth, and the part  $I_s$  returning through the overhead ground wires:

$$I_{fl} = I_s + I_{gg} \quad (2.2)$$

Furthermore,  $I_s$  is divided into current circulating through the overhead ground wires and tower footings at a short distance from the substation ( $\sum I_t$ ) and current returning along the shield wires  $(1-r)I_{fl}$  without causing any potential rises, i.e., the induced current.

$$I_s = I_t + (1-r)I_{fl} \quad (2.3)$$

where "r" is a factor indicating the proportion of the ground fault current that returns through the earth ( $I_g = rI_{fl}$ ). This factor is dealt with in Chapter 3.

Consequently:

$$I_f = I_{ft} + I_s + I_{gg}$$

$$I_f = I_{ft} + I_t + (1-r)I_{fl} + I_{gg}$$

$I_t + I_{gg}$  is the total current circulating in the earth ( $I_g$ ). This current could also include current circulating through additional ground conductors (i.e. neutrals, counterpoises, etc.), not shown in the figure for reasons of simplicity. Then:



$$I_f = I_{ft} + (1-r)I_{fl} + I_g \quad (2.4)$$

We note that by substituting  $I_g = rI_{fl}$  in equation (2.4) we go back to equation (2.1).

If more than one line enters the substation, and also carries zero-sequence currents, equation (2.1) becomes:

$$I_f = I_{ft} + \sum I_{fl} \quad (2.5)$$

At the design stage, it is difficult to determine how the fault current distributes among the grid of the substation and the other grounding conductors connected to it. Although faults in transmission lines are infrequent, and phase to ground faults in substations are rare (in this case the current magnitude can be large, owing to multiple infeeds from lines and generators), it is important to know the current flow for the purpose of calculating step and touch potentials, determining induction on neighboring circuits (i.e. telecommunication lines), and optimum setting of protective relays. Reference [12] gives a good review of the analytical methods available. Normally, a high current injection technique is used to measure this current distribution. Although there is no way to directly measure the portion of the test current that circulates into the ground grid only, if the circulating currents over the other ground conductors are measured, then the rest of the current will have to pass through the ground grid. Reference [15] outlines a procedure to establish the

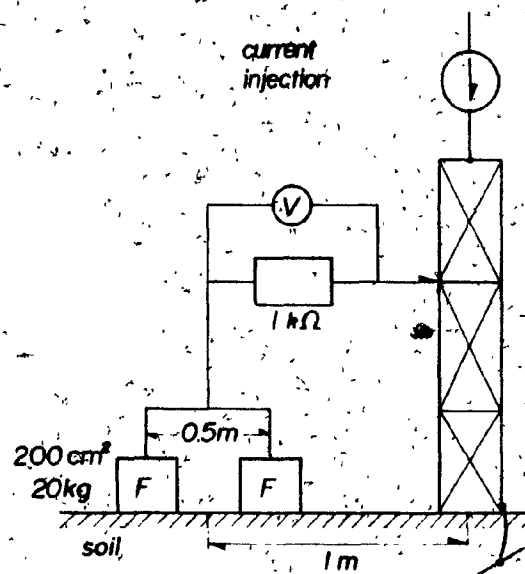
efficiency of each grounding element and to have a better picture of how the current distributes in the grounding complex, giving as well field tests results from the Bay James LG-2 powerhouse complex in Quebec.

### 2.3.2 Touch and Step Voltages.

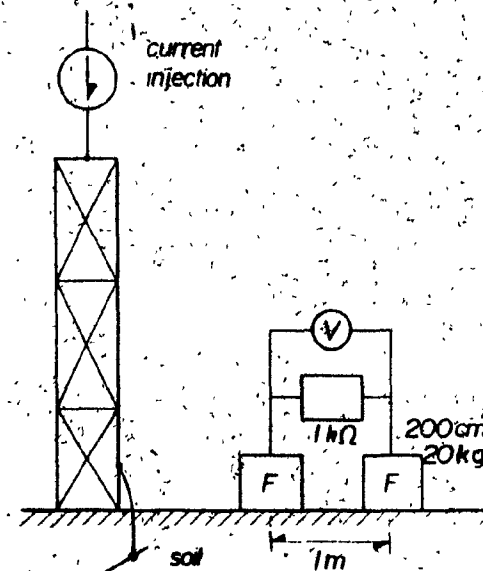
Touch voltage, as defined in reference [24], is the "potential difference between a grounded metallic structure and a point on the earth's surface separated by ... approximately one meter". Step voltage, on the other hand, is the "potential difference between two points on the earth's surface, separated by a distance of ... one meter, in the direction of maximum potential gradient".

As can be seen from the above definitions, the safety characteristics of a substation ground grid are determined by these two voltages, and their values have to be less than or equal to the tolerable potentials calculated with the IEEE Guide 80 formulas [23]. For an accurate measurement of step and touch potentials, an important condition to be fulfilled is to design and build test setups which take into account the influence of the various parameters on the measured values, namely, body resistance and contact resistance (between the feet and the soil). Reference [27] presents such a setup, using two electrodes to represent the influence of the feet, each weighing 20 Kg with an area of

200 cm<sup>2</sup> as recommended in [27]. The conventional resistance of the human body is represented by a one kilo-ohm resistance. Both setups are shown in fig. 2.4. Furthermore, reference [14] reports measurements in a transmission tower, using the above setups with injected currents of 1 and 1000 A. Results show that the low current injection can be used for safety evaluation of a grounding system.



(a)



(b)

FIGURE 2.4

Standard set-ups for measuring

a) Touch voltage and

b) Step voltage

## CHAPTER 3

### FIELD MEASUREMENT TECHNIQUES FOR SUBSTATION GROUND IMPEDANCE HIGH CURRENT INJECTION

#### 3.1 General.

The principle of high current injection methods is the same as the one described in the previous chapter. The test current ( $I_m$ )<sup>\*</sup> is injected through an overhead line connected to an auxiliary earth electrode at some distant point. This current probe could be the nearest substation or a transmission tower distant enough with a low resistance to earth. Preferably, and since the magnitude of the test current is dependent on the conductor impedance, all three phases of the injection line should be connected together in parallel, thus the impedance of the injection circuit becomes lower in comparison with the use of only one phase. Additionally, the reactance of the injection circuit can be further reduced by installing a series capacitor.

To inject the test current, a power circuit breaker is normally closed into a grounded phase, and various circuits can be used depending on the type of substation under study, for example:

- a) Use of a transformer from an auxiliary service.
- b) Use of a distribution circuit passing close to the

substation.

c) Use of a distribution circuit originating in the substation.

d) Use of a power transformer.

Preferably, a system independent from that used to supply customers should be used.

### 3.1.1 Current Measurement.

The test current can be conveniently measured with the current transformers (CT's) already installed on some substation equipment. If the objective is also to measure the current distribution in all grounding conductors, split-core CT's can be installed on these conductors, so as not to intentionally open ground circuits.

The potential rise caused by the current through the earth should exceed the residual voltage, therefore, a minimum test current in the order of 50-100 amperes is recommended.

### 3.1.2 Potential Measurement.

The potential rise of the grounding system under study is measured employing a voltmeter, an auxiliary conductor and a voltage probe sufficiently remote to reach the zero

earth potential. Attention should be paid to possible induction if this probe runs parallel to other energized lines. The potential probe can be an open wire line, a telecommunication cable or a temporary field cable. It is suggested to try different lengths and find out the point beyond which the result is about the same for at least three successive readings. A direct-reading phase angle difference meter, in conjunction with the voltage and current measurements, or a light beam oscillographic recorder, where all signals are printed simultaneously, is used to determine the ground impedance argument.

### 3.1.3 Shielding Factor.

Normally, the portion of the transmission line used for current injection will have one or two overhead ground wires. Consequently, the induced current on these wires should be accounted for. This is done by introducing the concept of "screening or shielding factor".

Due to the transfer of electromagnetic energy between a phase conductor and a neutral conductor (in this case an overhead ground wire), similar to the energy transfer in a transformer, a current ( $I_{in}$ ) will be induced by any test current carried by the line. This current is defined as:

$$I_{in} = I_m \frac{Z_{mw}}{Z_{sw}} \quad (3.1)$$

The current responsible for the voltage rise is given by:

$$\begin{aligned} I_g &= I_m - I_{in} \\ &= I_m \left( 1 - \frac{Z_{mw}}{Z_{sw}} \right) \end{aligned}$$

$$I_g = (r) I_m \quad (3.2)$$

where "r" is the screening or shielding factor.

In short, the shielding factor is an indication of the share of the test or fault current which flows through the substation ground impedance. This shielding factor is normally calculated, although under certain situations it is advisable to determine it experimentally (for example, if the overhead line has mixed type shield wires).

### 3.2 Synchronous Power-Frequency Method.

In this method, the power-frequency injected current is normally fed through a transmission line conductor from a low voltage network or a separate transformer with polarity reversal and regulation capabilities. A single phase transformer with secondary tapings will generally do the job. A series capacitor could be used to reduce the need to



supply reactive power, and thus decrease the transformer size.

If an initial current ( $I_i$ ) exists in the injection line when the source of  $I_m$  is short-circuited, the same must be measured together with the corresponding initial voltage ( $V_i$ ). To minimize errors caused by  $I_i$  and  $V_i$ , these quantities should be measured before and after injecting  $I_m$ . Besides, it is necessary to measure the total currents  $I_{ma}$  and  $I_{mb}$  and potentials  $V_{ma}$  and  $V_{mb}$  with  $I_m$  injected in both polarities (see figure 3.1) [42].

The values of  $V_{ma}$  and  $V_{mb}$  include the residual voltage (see figure 3.2), which should not be considered when determining the ground impedance. From figure 3.2, we note that:

$$V_m - (-V_i) = V_{ma} \quad (3.3)$$

$$-V_m - (-V_i) = V_{mb} \quad (3.4)$$

With the aid of the phasor diagram in figure 3.3 we have, using the cosine law: (in the following equations, up to 3.10, only magnitudes are dealt with)

$$V_{ma} = \sqrt{V_m^2 + V_i^2 - 2V_m V_i \cos \alpha} \quad (3.5)$$

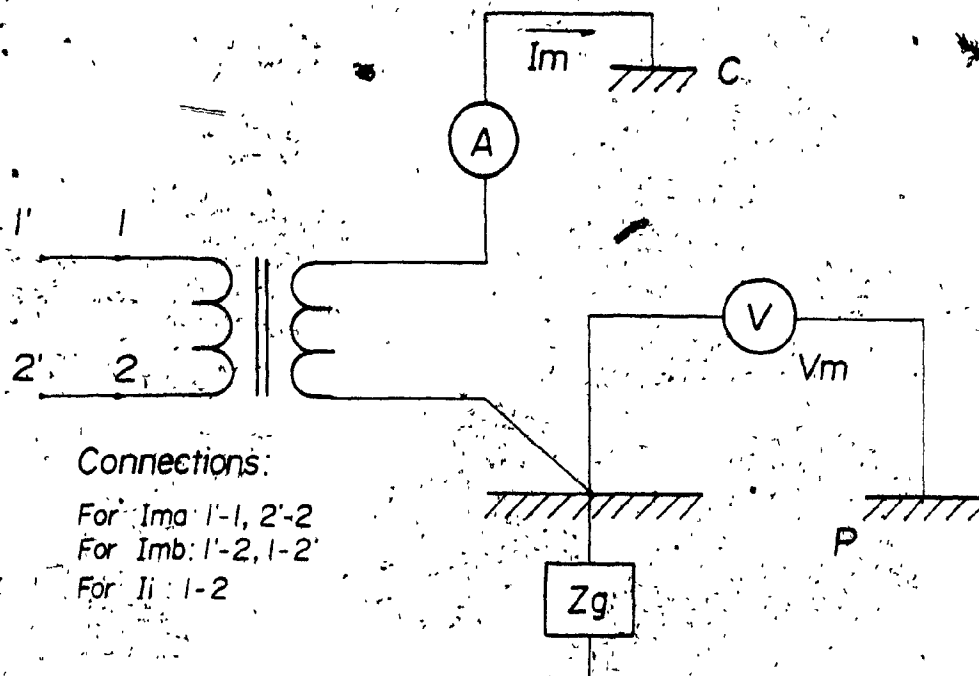


FIGURE 3.1

General lay-out of the synchronous  
power-frequency method

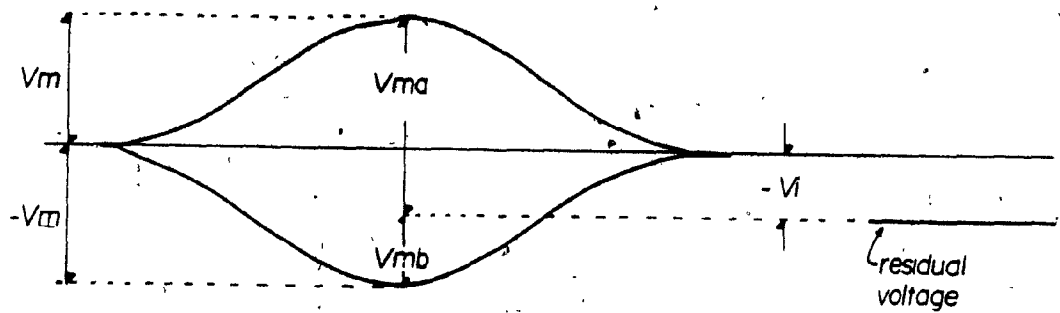


FIGURE 3.2

Potential rise measurement with both polarities

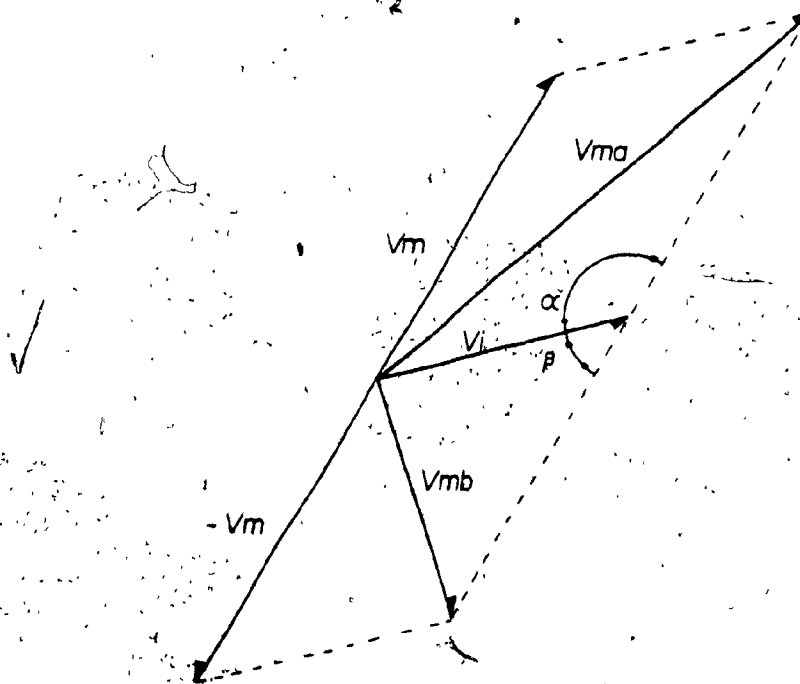


FIGURE 3.3

Phasor diagram of measured and residual voltages

$$V_{mb} = \sqrt{V_m^2 + V_i^2 - 2V_m V_i \cos \beta} \quad (3.6)$$

If we square both previous equations and add them:

$$V_{ma}^2 + V_{mb}^2 = 2V_m^2 + 2V_i^2 - 4V_m V_i (\cos \alpha + \cos \beta) \quad (3.7)$$

Noting that  $\alpha + \beta = 180^\circ$ :

$$\cos \alpha + \cos \beta = 2 \cos \frac{1}{2}(\alpha + \beta) \cos \frac{1}{2}(\alpha - \beta) = 0 \quad (3.8)$$

Solving for  $V_m$ , and writing a similar equation for the current:

$$V_m = \sqrt{\frac{V_{ma}^2 + V_{mb}^2}{2} - V_i^2} \quad (3.9)$$

$$I_m = \sqrt{\frac{I_{ma}^2 + I_{mb}^2}{2} - I_i^2} \quad (3.10)$$

Finally, the ground impedance that we are looking for is:

$$Z_g = \frac{V_m}{(r) I_m} = \frac{1}{r} \sqrt{\frac{V_{ma}^2 + V_{mb}^2 - 2V_i^2}{I_{ma}^2 + I_{mb}^2 - 2I_i^2}} \quad (3.11)$$

where "r" is the shielding factor of the transmission line, and is introduced to account for the induced current in the overhead ground wires. If true rms instruments are used

with this polarity reversal method, the effect of harmonics truly disappears [13], but the magnitude of the test current and associated potential rise should exceed the interference level, since it is assumed to be steady. Some companies in Europe use an automatic changeover device for building the circuits to measure  $V_{ma}$ ,  $V_{mb}$ , and  $V_i$  for various test current periods (e.g. 20s, 50s, and 5s, respectively) [13].

### 3.3 Interference Compensation Method.

This is also considered a synchronous method. It uses power-frequency injection current and compensates the power-frequency residual voltage to zero with the injection circuit open [28]. This compensation is achieved by a separately adjustable voltage source both in magnitude and in phase angle, ( $-V_C$ ) or two independent adjustable perpendicular voltage sources (see Figure 3.4).

After the compensation, the test current is injected by means of a transformer or an ac generator and the instruments will then measure the required values. In order to successfully apply this method, a frequency-selective voltmeter should be used to read the potential rise, or else strong harmonics could interfere with the measurement. Since this method also presupposes a steady interference level, the interference voltage measurement should be made

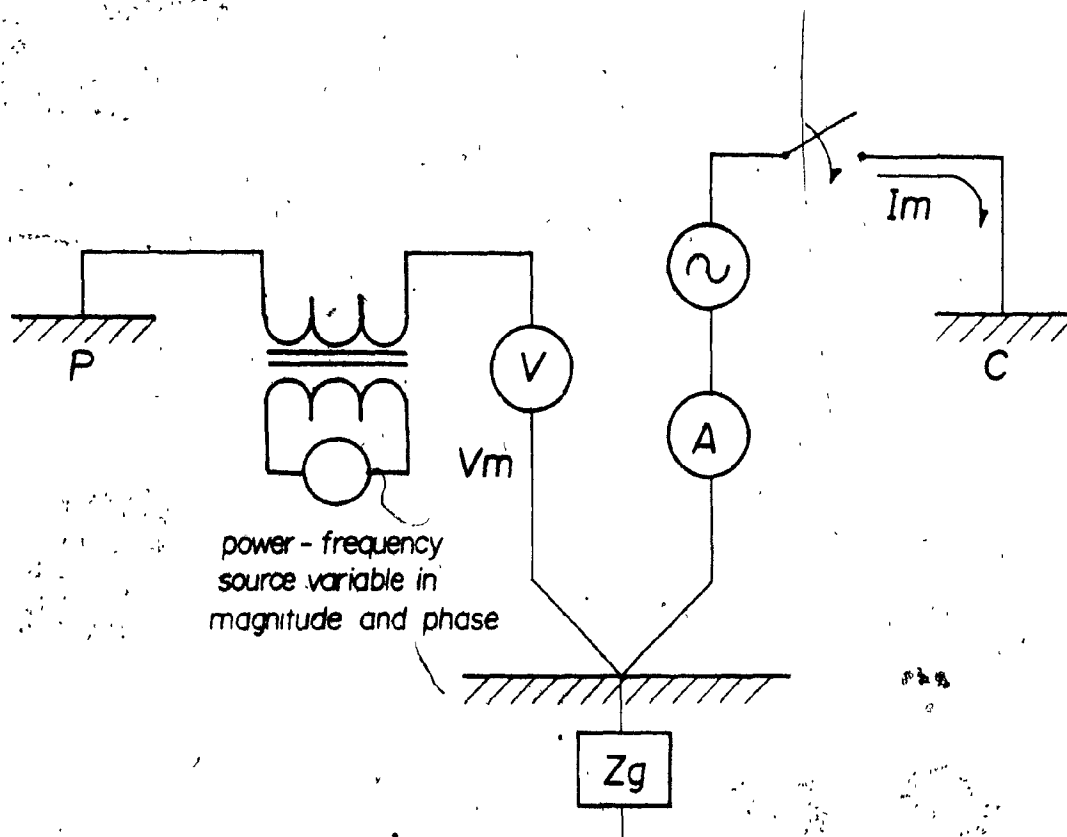


FIGURE 3.4

General lay-out of the interference  
compensation method.

before and after the current injection.

If current is injected with only one polarity ( $I_{ma}$ ), an alternative method could be to measure the magnitude and phase angle with the test circuit open, and then subtract it from the measured value:

$$V_m = V_{ma} - V_c \quad (3.12)$$

### 3.4 Beat-Frequency Method.

This method involves an asynchronous test current, which needs a separate power supply (see figure 3.5). Usually, a mobile ac generator with a frequency 0.1 to 0.5 Hz above or below the power-frequency is used [28]. Due to the frequency difference between the injected current ( $I_m$ ) and the interference caused by the network in normal operation, the beat-frequency maxima and minima will occur in the test line as well as in the measured potential. Provided the instruments used have a fast response time, the values of the maxima and minima ( $I_{max}$ ,  $V_{max}$ ,  $I_{min}$ ,  $V_{min}$ ) are measured, then the injected current and voltage rise is calculated as the mean of the maximum and minimum instrument readings: (The following equations, up to 3.15, are in magnitude only)

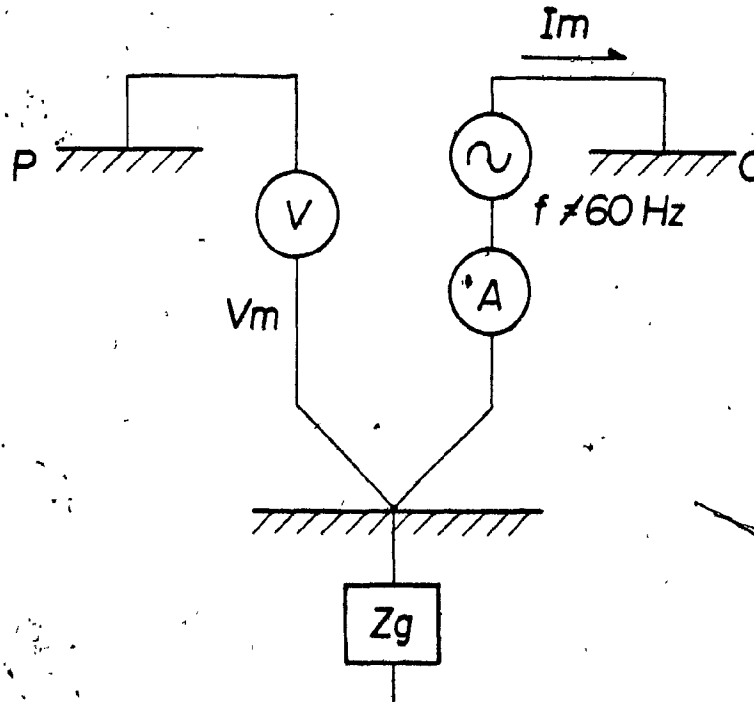


FIGURE 3.5  
General lay-out of the  
Beat-frequency method



$$I_m = \frac{1}{2}(I_{\max} + I_{\min}) \text{ for } I_m > I_i \quad (3.13)$$

$$V_m = \frac{1}{2}(V_{\max} + V_{\min}) \text{ for } V_m > V_i \quad (3.14)$$

$$I_m = \frac{1}{2}(I_{\max} - I_{\min}) \text{ for } I_m < I_i \quad (3.15)$$

$$V_m = \frac{1}{2}(V_{\max} - V_{\min}) \text{ for } V_m < V_i \quad (3.15)$$

$$Z_g = (-) \frac{1}{r} \frac{V_{\max} \pm V_{\min}}{I_{\max} \pm I_{\min}} \quad (3.17)$$

The residual voltage and current ( $V_i$  and  $I_i$ ) should also be measured before and after injecting the test current, but for the sole purpose of knowing which formulas to apply.

### 3.5 Frequency Different from Power-Frequency Method.

To use a frequency different from the power-frequency, at least 5 Hz difference is recommended, and that the measuring instruments are of the selective type. This method avoids power-frequency interference, but a deviation of more than 10 Hz can introduce a significant error when overhead ground wires or cable shields have an important contribution to the grounding system, since they will introduce a reactive component that will vary with frequency.

An example of this method is given in reference [9], where measurements were performed at a complex containing two nuclear electric plants. A current signal slightly offset from power frequency was injected into selected lines (the remotely grounded point ranging in distance from 0.5 to 100.0 km), while normal power transmission was maintained on the remaining lines. On the longer lines (10 and 100 km), all three phases were energized in parallel to minimize circuit impedance. The faulted lines were energized using a gasoline-powered ac welding set capable of supplying up to 20 kW, and adjusted for an output frequency of 58 Hz.

Additionally, a step-up transformer was used to improve the impedance match. On the remaining circuits (less than 10 km) and in order to simulate the impedance characteristics of a single-line-to-ground fault, only one phase conductor was connected. The objective of these measurements was mainly to determine the transfer impedance between communication and control cables and the local ground, in order to calculate the voltage stresses on these cables in the event of a line to ground fault, taking into account each transmission line segment contributing to the fault. The measured quantities were the amplitude and phase of the fault-produced voltages and currents relative to the injected current. These quantities were extracted from the power-frequency interference by first passing the test signal through a 60 Hz notch filter, adjusted to reduce the

interference by a factor of up to 100. Then, with the aid of a dual-channel oscilloscope, a phase-locked oscillator was adjusted in amplitude and phase, until the "beat" of the 8 Hz frequency offset disappeared. This indicated that the output of the oscillator was equal in magnitude and in phase to the 68 Hz test signal (figure 3.5). This procedure was used to measure both the current and voltage signals. The ratio of the two results gave the test impedance with the error in magnitude and phase cancelling in the notch filter.

### 3.6 Safety During Field Measurements.

As pointed out earlier, grounding tests with injected current in the order of tens or hundreds of amperes represents a dangerous situation and every effort should be made to minimize the risk of possible hazards.

In general, these safety rules should be kept in mind and followed:

a) Extended test leads or out-of-service transmission lines present a high degree of exposure to atmospheric disturbances. Consequently, power system grounding tests should not be scheduled, or should be stopped if already underway, during periods of lightning activity.

b) When tests are not in progress, all external laid out field cables should be opened and isolated from the grid.

During testing, cables used to measure the voltage rise should be considered live at all times and over their entire length.

c) The HV line used for current injection must be earthed at both ends when the test is under preparation. The injection end cannot be grounded during the actual measurement, but a safety spark gap with a sparkover voltage of 2-3 kV is advisable at the line entrance, in view of atmospheric overvoltages or inadvertent energizing of the line.

d) Measuring instruments should be connected to the injection circuit through instrument transformers or resistance voltage dividers.

e) All personnel present in the substation under study must be informed of the nature of the tests, and in particular of the consequences of current circulating in the ground.

f) A test sequence should not be considered terminated until the opening of the test circuit is confirmed visually.

g) Applicable state or national safety electric codes should be followed.

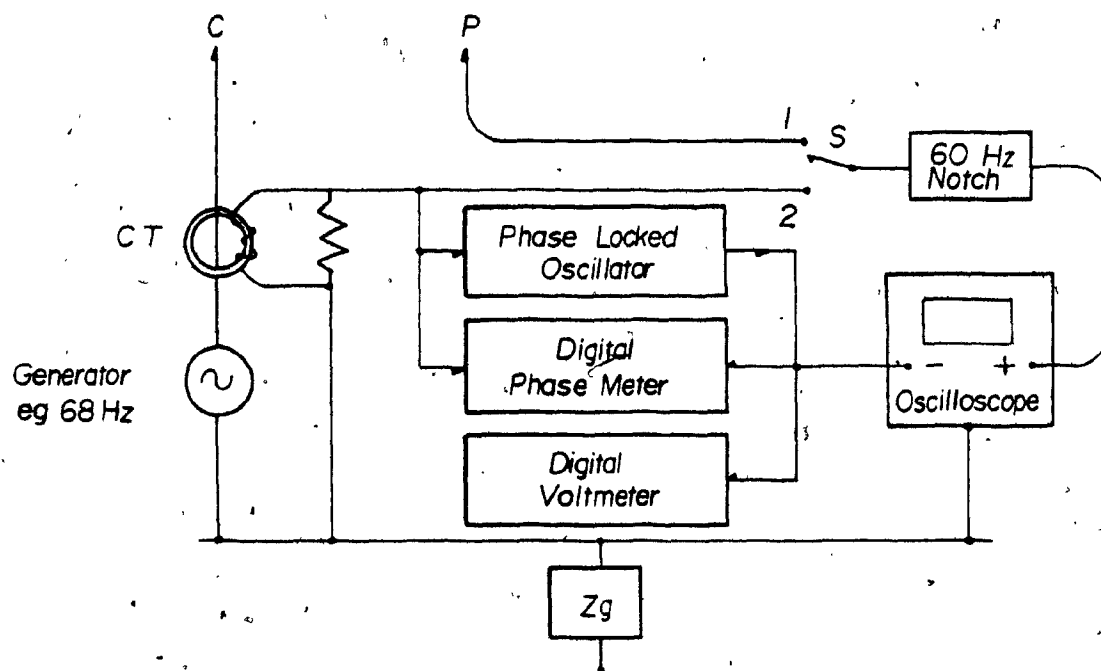


FIGURE 3.5

Method of measuring test signals  
in presence of 50 Hz interference.

## CHAPTER 4

### FIELD MEASUREMENT TECHNIQUES FOR SUBSTATION GROUND IMPEDANCE

#### LOW CURRENT INJECTION

##### 4.1 General.

The principle of low current (LC) injection methods is the same as the one described in Chapter Two. The test current ( $I_m$ ) is normally injected through a temporary field cable or a telecommunication line. The use of a phase conductor in a transmission line is not recommended since contact resistances (e.g. between overhead ground wires and towers) or ferromagnetic paths (e.g. steel ground wires, steel armoured cable sheaths, etc.) in the ground electrode system at or near the injection line may introduce non-linearities (dependency on current or voltage, [28]), yielding pessimistic results up to 70 per cent higher measured impedance, (see figure 4.1).

All of the existing techniques to measure ground impedance with low current injection use ac currents at frequencies different from 50 or 60 Hz, or else residual voltages resulting from unbalanced power system currents would surely interfere with the potential measurement. This also implies the use of a frequency-selective detector in the auxiliary potential lead.

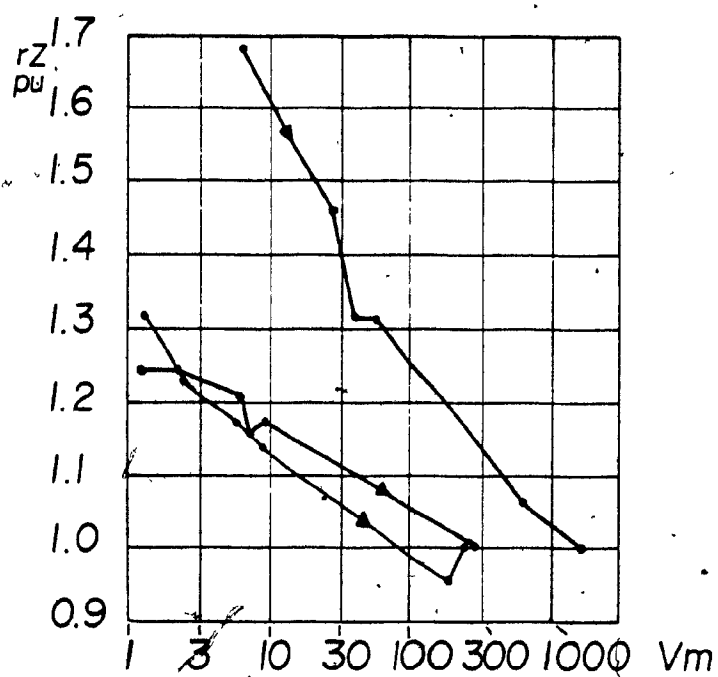


FIGURE 4.1

Dependence of the product of ground impedance  
and screening factor upon increasing test  
voltage at three 110 kV substations [28]

#### 4.2 Oscillator-Voltmeter Method.

This technique was developed using an ac signal close to 60 Hz to measure  $Z_g$ . The value measured represents the Thevenin equivalent impedance of all series and parallel paths that exist between the substation grid under test and remote earth. The 60 Hz impedance is taken to be the same as that measured at the test frequency.

An example of this method is presented in reference [29] and illustrated in Figure 4.2. The instrumentation scheme consisted of the following items:

- a) Tuneable sine-wave power oscillator for the current source, capable of 100 W output.
- b) High input impedance frequency-selective voltmeter as the detector.
- c) Telephone cable pairs as the current and voltage probes.
- d) A 60 Hz rejection filter at the ~~voltmeter~~ input, when required.

A summary of the measuring procedure of reference 29 is as follows:

- 1) Set the instruments as shown in figure 4.2. Voltage and current auxiliary probes should reach remote earth.
- 2) With the voltmeter connected to the voltage probe, scan the frequency band around 60 Hz to find a low noise "window"



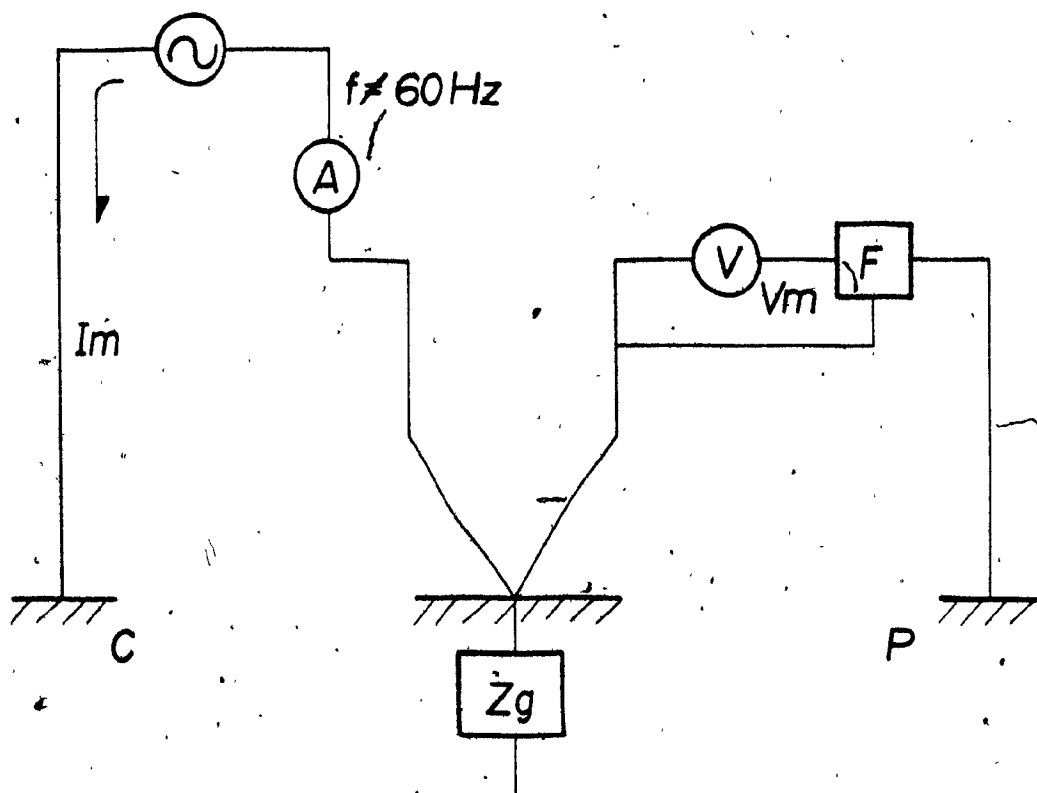


FIGURE 4.2  
General lay-out for the  
Oscillator-voltmeter method

in the ambient noise. Such a window was found, for this particular case, in the range of 55-68 Hz.

3) Set the oscillator frequency to that found in the previous step and adjust the output to the selected current (0.5 A in this case).

4) Tune the frequency-selective voltmeter to the oscillator frequency and read the voltage on the voltage probe resulting from the oscillator current. (A 60 Hz rejection filter may be required ahead of the voltmeter if the voltage probe has a high ambient 60 Hz on it).

5) Repeat steps 1) thru 4) for other P locations until an asymptotic value of  $Z_g$  has been obtained. (As discussed in Chapter 2).

One disadvantage in this method is that the phase angle of the ground impedance cannot be obtained.

#### 4.3 Portable Instrument for Ground Impedance Measurements

[34].

This instrument (still in the experimental stage, not yet commercially available) is capable of measuring low impedances in the presence of high interference (20 V). The instrument drives a known ac current through the grounding system and measures the in-phase and quadrature components (with the use of a phase-sensitive detector) of the fall-of-potential method, and displays these voltages as resistance and reactance. By using a sine wave test current

the measurements are made at four fixed frequencies, three of them above, and one below the power-frequency (36.47, 85.33, 128.00, and 146.00 Hz). The instrument is designed to measure from  $2 \Omega / 2\text{mH}$  full scale up to  $20 \text{ k}\Omega / 200 \text{ mH}$  full scale.

At each potential probe location, measurements are made of the resistance and reactance at each of the four frequencies, which means a total of eight readings at each location. If the display is noisy, the instrument has a filter that can be switched on to help smooth the reading. The impedance at the power frequency is obtained by interpolation. The output voltage is limited to 50V for personnel safety, and the battery size limits the current to 10 mA.

An example of the step-by-step procedure using this instrument is presented in reference [35], from measurements taken in an 80 by 80m distribution substation in the city of Guadalajara, Mex. The current probe (C) was located 400m away from the substation, and the potential probe (parallel to C) run in 20m steps (beginning at 50m). The measurements were performed as follows:

- a) At each P location, the readings from X and R were procured, at each of the four frequencies.
- b) When all readings in a) were taken (up to a distance of 190m for P), the 50 Hz value was interpolated at each P.

location, both for the resistance and reactance readings (see figure 4.3).

c) With the 60 Hz resistance values, the  $R_g$  vs.  $P$  curve was built, as shown in figure 4.4. If the distance to the current electrode is enough, then the flat portion of this curve indicates the substation ground resistance (in this case  $355 \text{ m } \Omega$ ).

d) For the reactance values, the mutual inductance between the test leads has to be accounted for. This problem is addressed in reference [45] and later on in this thesis. After the mutual coupling is removed, the curve  $X$  vs.  $P$  is built (figure 4.4). For comparison purposes, this figure also presents the reactance value with the mutual coupling present. Theoretically, a mutual ac resistance is also present, although in this example it was negligible. Note that after the mutual effect is removed, the reactance curve shows a flat portion.

e) Finally, the ground impedance was calculated to be  $Z_g = 355 + j200 = 407 / \underline{29} \text{ m-ohm}$ .

#### 4.4 Frequency-Scanning Method.

In the previous two methods, the ground impedance is either interpolated from measurements at fixed frequencies, or the 50 Hz impedance is taken to be the same as that obtained at the test frequency. The purpose of this method, first reported in [32], is to avoid possible errors when the

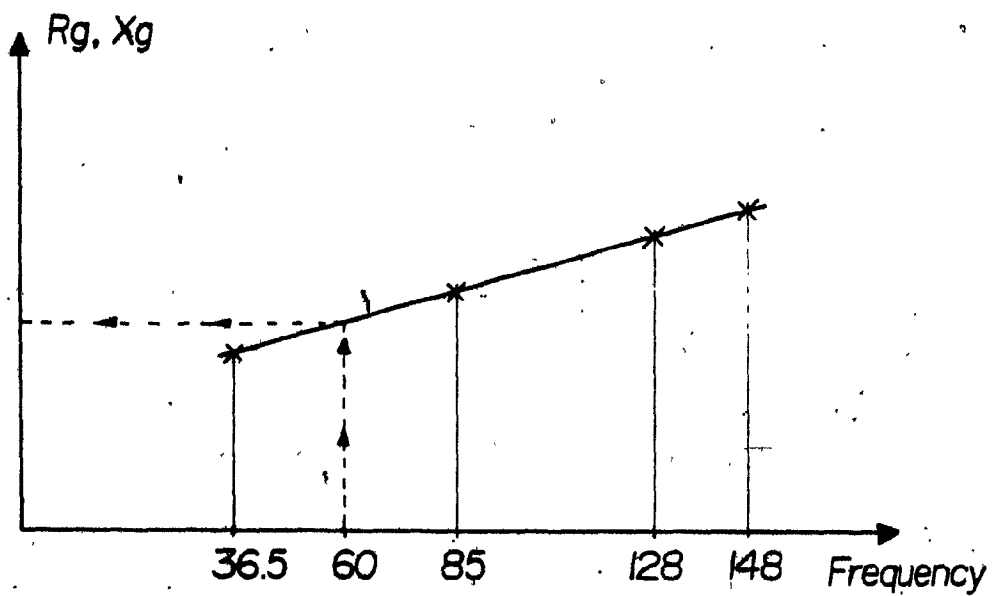


FIGURE 4.3

Plot of  $R_g$  (or  $X_g$ )  
against frequency

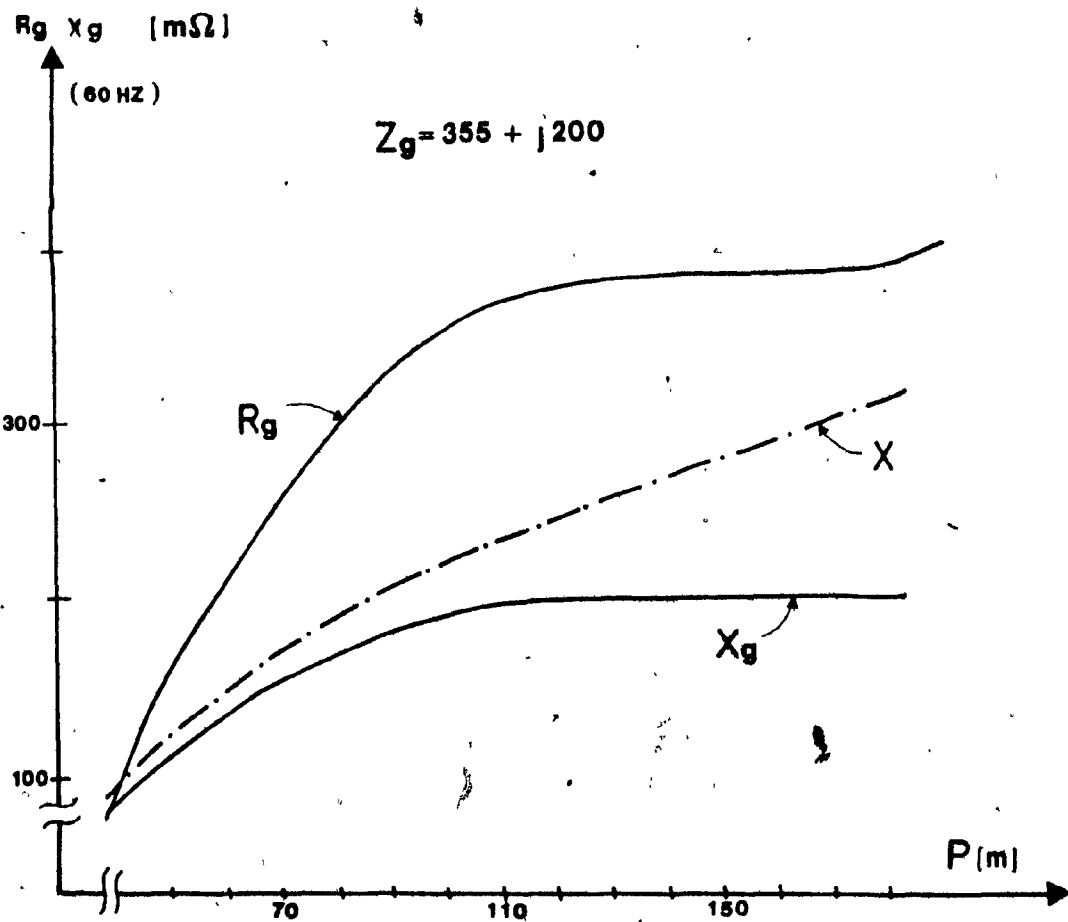


FIGURE 4.4

Plot of ground impedance vs. distance  $P$   
at Tesistan Substation

ground impedance does not vary smoothly with frequency.

This technique allows for a complete plot of impedance and phase angle over a wide frequency range. The signal source consists of a pseudorandom noise generator, a noise conditioning filter and a power amplifier of about 1.5 kW (see figure 4.5). The output of the power amplifier must be high enough to produce a voltage change in the grounding system under test, larger than the residual ground system voltages due to power system unbalanced currents, and to the background random voltage present at frequencies other than the power-frequency or its harmonics. The bandwidth of the noise source was set from 0 Hz to 400 Hz. An external filter was used to limit the noise signal to a range of 10 to 400 Hz in order to protect the power amplifier output transformer and the power transistors from the effects of low frequency saturation. The digital signal analyzer must be a dual channel instrument.

With the instruments set up as shown in figure 4.5, the current and voltage signals were first filtered, then digitalized and transformed in the frequency domain through an FFT (Fast Fourier Transform) routine. Using the transfer function of the spectrum analyzer, the display (either CRT or X-Y plotter), will show the impedance magnitude and phase over a selected frequency range. The existing background power system voltages in the grounding system lead to strong

peaks on the transfer impedance diagram at 60 Hz and its odd harmonics. However, these are ignored as it may be assumed that the magnitude and phase curves would be smooth without the presence of these residual voltages, and  $Z_g$  at 60 Hz is found by interpolation. The FFT analyzer is programmed to make repeated measurements, which are added and averaged several times to reduce the effects of external noise.



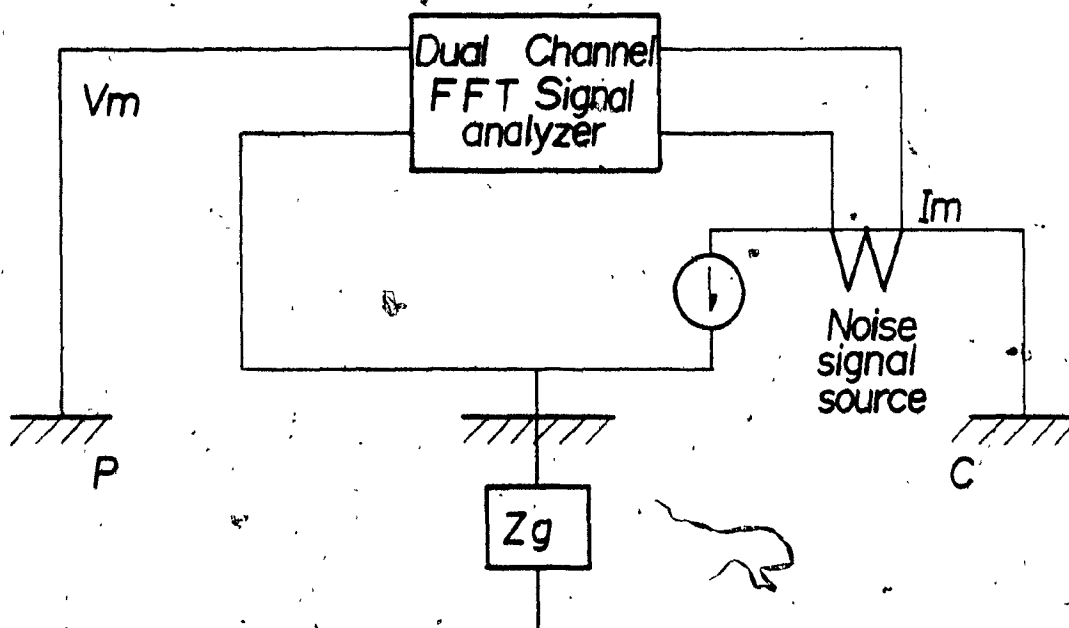


FIGURE 4.5  
General lay-out  
for the frequency-scanning method.

## CHAPTER 5

### COMPARATIVE FIELD MEASUREMENTS WITH HIGH AND LOW CURRENT INJECTION METHODS

#### 5.1 Introduction.

In 1981, as a result of a collaborative program with Hydro-Quebec, this author formed part of the team that went to the field and conducted a series of ground impedance measurements at a distribution substation called Yamaska, and at a power substation called Becancour.

Yamaska has an area of approximately 4000 m<sup>2</sup> and is located in a rural area surrounded mostly by corn fields. There is one 120 kV transmission line coming in and out of the substation, and several 25 kV distribution feeders originate from it (see figure 5.1). The main purpose of these tests was to compare high and low current injection methods.

For the high current testing, a power transformer with a secondary voltage of 25 kV was used to inject current magnitudes in the order of 500 A through the 120 kV line. For the low-current testing, the frequency-scanning method described in [32] was used. Because measurements with the latter method were taken at different angles between the

potential and current leads, the effects of mutual coupling were clearly observed, with the opportunity to further substantiate the equations developed in [45].

All ground impedance measurements were performed with the grounding system in its normal operative configuration, that is, keeping all external connections (overhead ground wires, counterpoises, distribution neutrals, etc.) in place.

## 5.2 Resistivity Measurements.

Published work by Tagg [45] shows that the earth impedance of an electrode is largely determined by the components at the periphery of the system. Accordingly, a soil resistivity survey [48] was taken with a digital earth tester, as close to the site perimeter as possible. Experimental data has also shown that the earth cannot usually be regarded as a uniformly conducting medium [43]. Two-layer formulas have been found to give satisfactory results, and its use nowadays is widely spread. Therefore, the results of the resistivity survey were fed into a computer program in order to obtain the two-layer model [19] with the following results:

First layer resistivity = 28.1  $\Omega$ -m

Second layer resistivity = 25.5  $\Omega$ -m

Height of first layer = 8.9 m

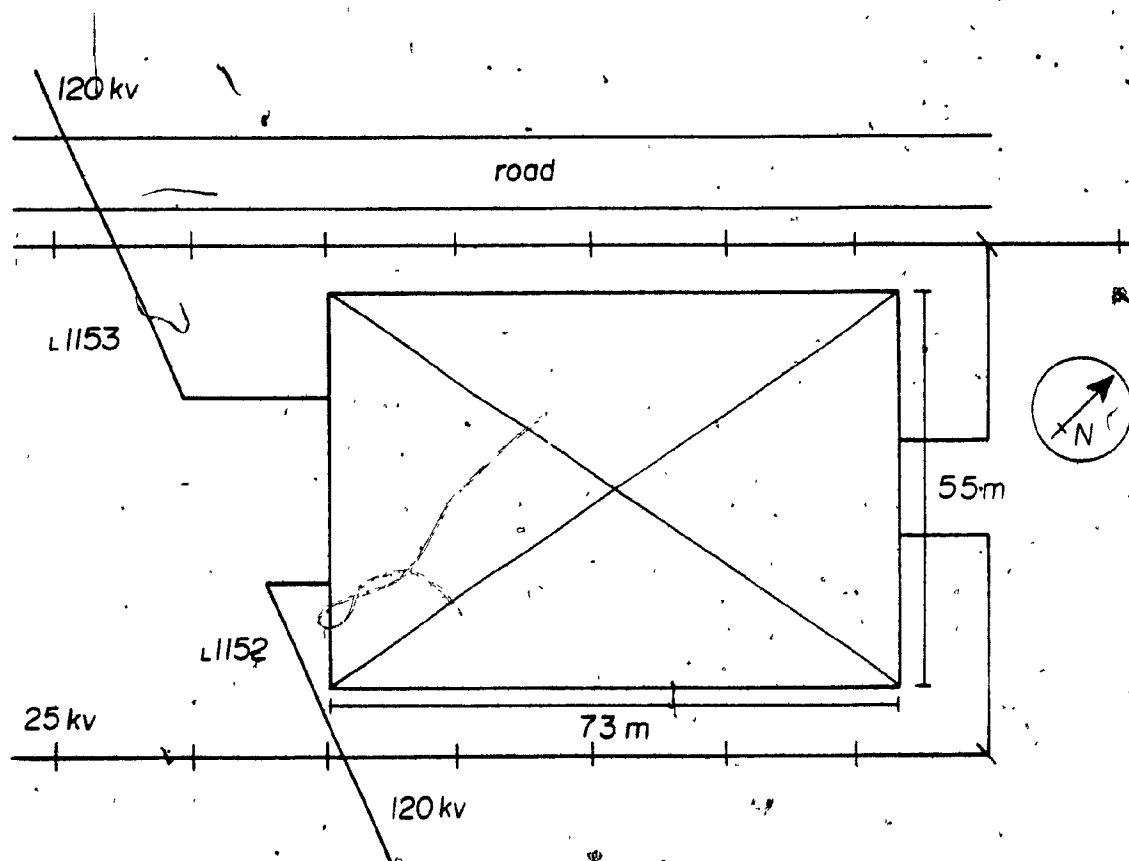


FIGURE 5.1

Hydro-Quebec's Yamaska substation

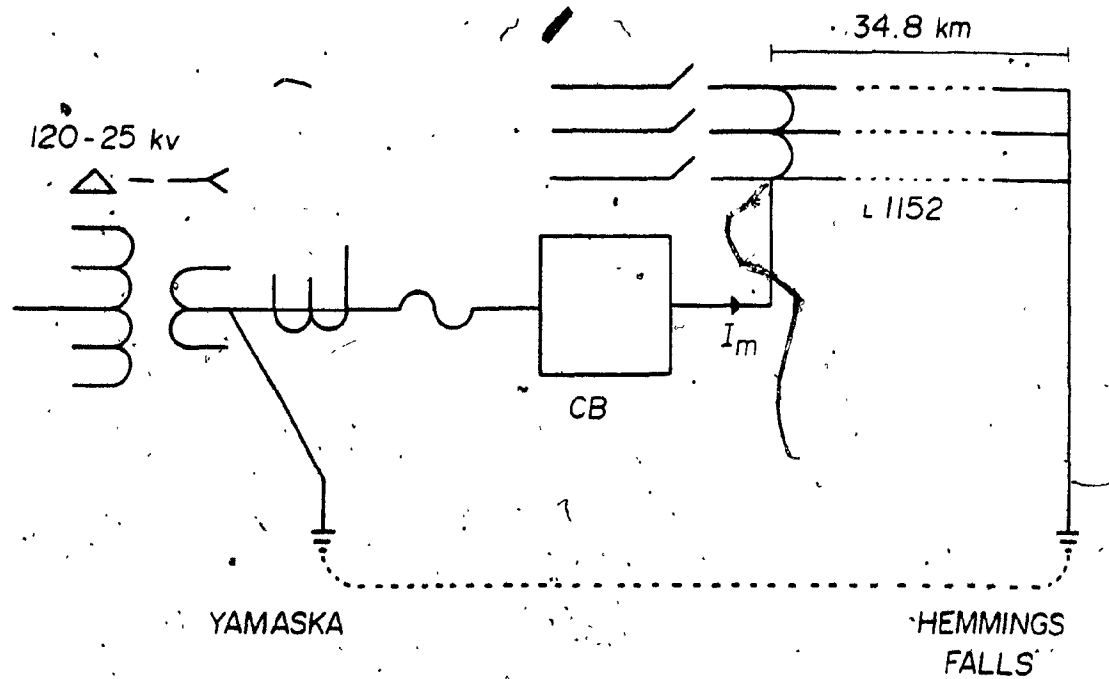


FIGURE 5.2  
Short circuit testing set-up

The equivalent resistivity was determined from the curves shown in Chapter 2 of Sunde [43]. This value of 28 ohm-m was used in the calculations of both the mutual coupling effects between auxiliary leads and the shielding factor of the line feeding the test current.

### 5.3 High Current Method and Results.

The test current was injected via the 120 kV line with its three phases connected in parallel to further reduce its impedance, and grounded at the nearest substation (Hemings Falls), conveniently chosen as the auxiliary current electrode (C), located 35 km away from Yamaska. Current injection ( $I_m$ ) was possible by means of a power transformer with a secondary voltage of 25 kV. A simplified diagram of the test circuit is shown in figure 5.2. The purpose of the circuit breaker was to limit the short circuit duration to 10 cycles of the 60 Hz.

The potential rise ( $V_m$ ) was measured with potential probes at three points, extending away from the substation by means of temporary field cables, laid out at an angle of 90 degrees with respect to the 120 kV line used for current injection (figure 5.3).

Both current ( $I_m$ ) and voltage ( $V_m$ ) signals were displayed in an oscillographic recorder, which allowed for

the calculation of the ground impedance magnitude and its phase angle. The average magnitude of the test current was 591 A, (Appendix D elaborates in more detail on how this current magnitude was arrived at), and the following table shows the measured ground impedance, with figure 5.4 displaying the corresponding curve:

TABLE 5.1

	P (m)	Z (m $\Omega$ )
P1	1310	113 <u>/5</u>
P2	1490	115 <u>/15</u>
P3	1830	115 <u>/3</u>

From figure 5.4 it can be stated that the measured ground impedance has a value of 115/9 (m  $\Omega$ ). The phase angle was taken as the average of the last two measurements. Nevertheless, the induced current in the ground wires of the test line has to be taken into account. The final ground impedance is given by:

$$Z_g = \frac{V_m}{r I_m} \quad \Omega \quad (5.1)$$

where "r" is the screening factor defined in Chapter 3. For this particular line it was calculated: (Refer to Appendix C)

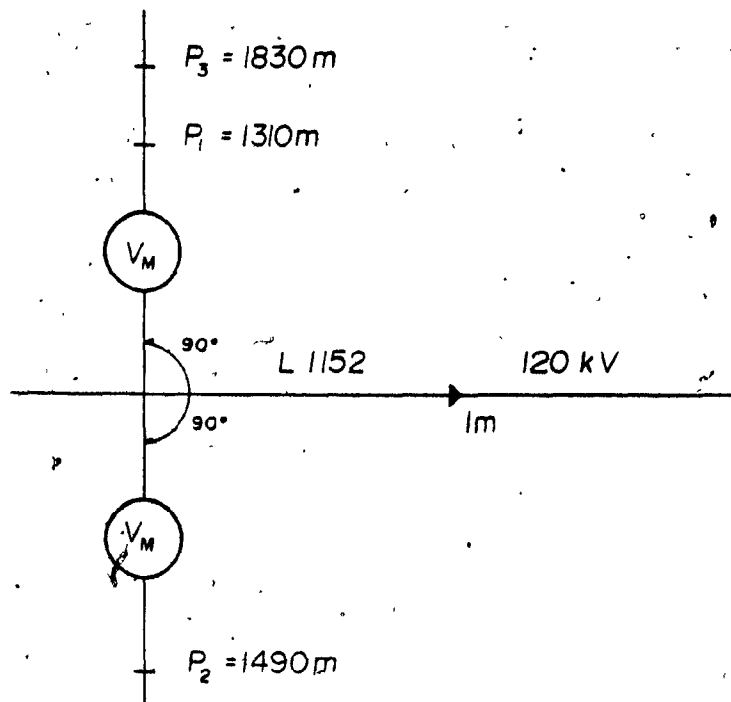


FIGURE 5.3

Potential probe locations for High Current injection

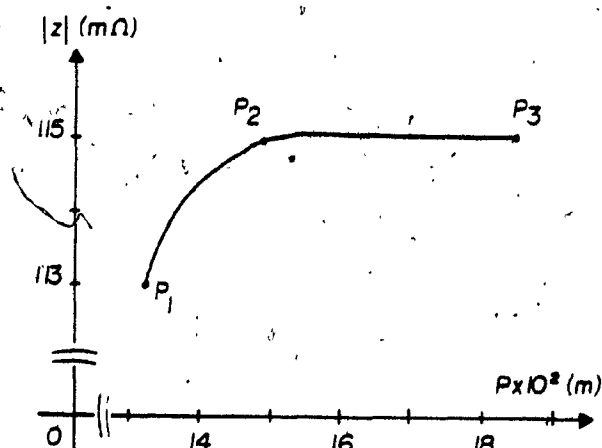


FIGURE 5.4

Ground impedance profile in High Current testing



$$r = 0.924 \angle -7 \quad (5.2)$$

Consequently, the final ground impedance is:

$$Z_g = \frac{115 \angle 9}{.924 \angle -7} = 124 \angle 16 \text{ m}\Omega \quad (5.3)$$

#### 5.4 Low Current Injection Method.

##### 5.4.1 Instrumentation.

A similar procedure as the one described in the frequency-scanning method was selected. Figure 5.5 is an schematic diagram of the configuration employed. The current was injected by means of a sweep generator and amplified with a power source. After some testing was done, the current chosen for injection had the following characteristics: 4 A, 0.15 s sweep from 20-250 Hz. Both the voltage and the current signals (P and C) from the auxiliary probes were recorded and processed by a digital signal analyzer equipped with a Fast Fourier Transform (FFT) routine. The result is a transfer impedance diagram with information about the magnitude and phase of the ground impedance in the specified frequency range. A typical transfer diagram is pictured in figure 5.6.

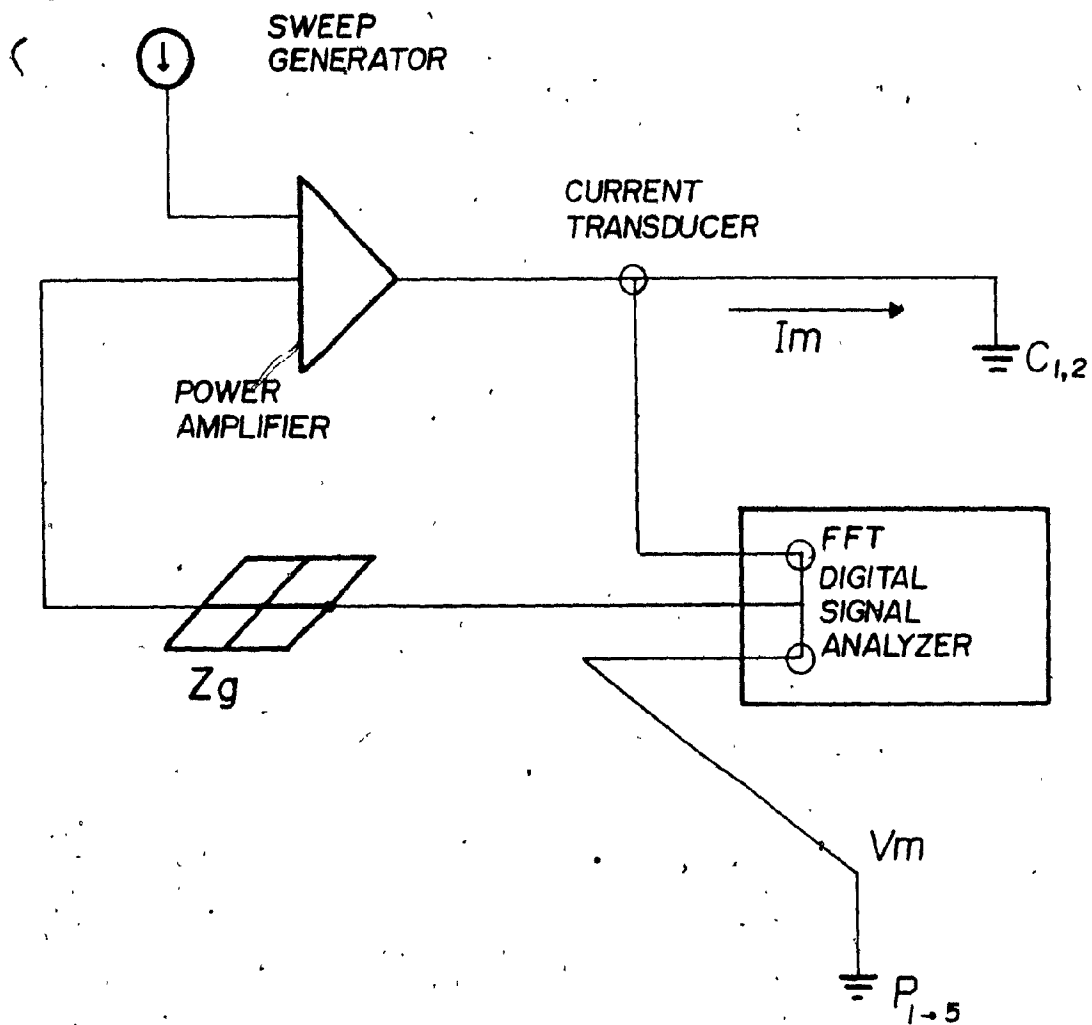


FIGURE 5.5

Low Current injection circuit

#### 5.4.2 Measurement Points.

In the application of the low current method, both the potential and the current auxiliary electrodes were installed by means of temporary field cables extended away from the substation. Figure 5.7 shows the different directions in which potential probes were installed with respect to two current injection points ( $C_1$  and  $C_2$ ).  $P_1$  to  $P_5$  show the directions in which the potential readings were taken. In this way, measurements were taken at the following angles:

$\theta=0$  (direction  $P_1$  with current injected at  $C_1$ ).

$\theta=45$  (direction  $P_2$  with current injected at  $C_1$ ).

$\theta=90$  (direction  $P_3$  with current injected at  $C_1$ ).

$\theta=95$  (direction  $P_4$  with current injected at  $C_2$ ).

$\theta=140$  (direction  $P_5$  with current injected at  $C_2$ ).

This does not mean that only one reading was procured at each angle. Two examples will show the procedure followed.

#### 5.4.3 Analysis of Field Measurements.

a) Example with  $\theta > 90$  degrees.

The following example will illustrate the manner in which the ground impedance magnitude at 60 Hz was determined

for each potential probe direction ( $P_1$  to  $P_5$ ). Let's take direction  $P_5$  which makes an angle of 140 degrees with respect to the injection circuit  $C_2$ . In this direction a total of five measurements were obtained at increasing distances as shown in table 5.2.

TABLE 5.2

P (m)	Z ( $m\Omega$ ) at 50 Hz
229	95 $\angle 15$
343	109 $\angle 15$
457	121 $\angle 15$
497	121 $\angle 15$
610	115 $\angle 15$

At each of the measurement points indicated previously, a transfer impedance diagram in the frequency domain was obtained from the spectrum analyzer, suchlike the one shown in figure 5.6. The upper curve shows the ground impedance phase angle, while the lower one displays the ground impedance magnitude in a frequency range from 20 up to 250 Hz. From these diagrams, the 50 Hz value was determined as accurately as possible by interpolation, obviously ignoring the peaks. After this was done, the next step was to remove the mutual coupling effect from each of the five values in

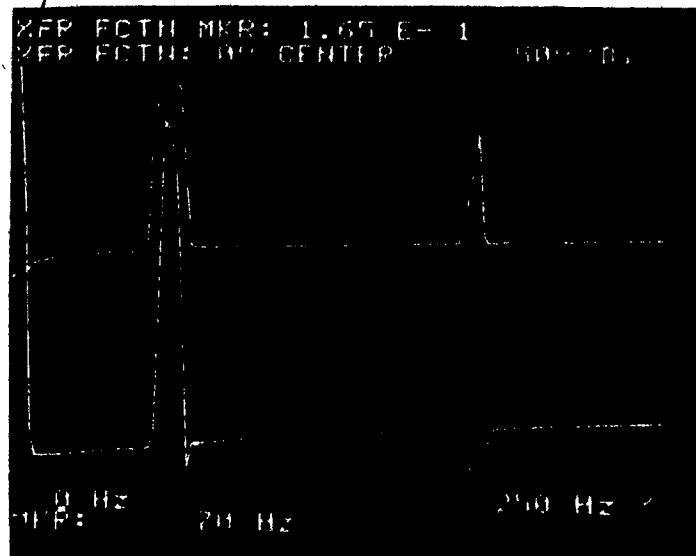


FIGURE 5.5

Upper curve: Transfer impedance phase angle

Lower curve: Transfer impedance magnitude

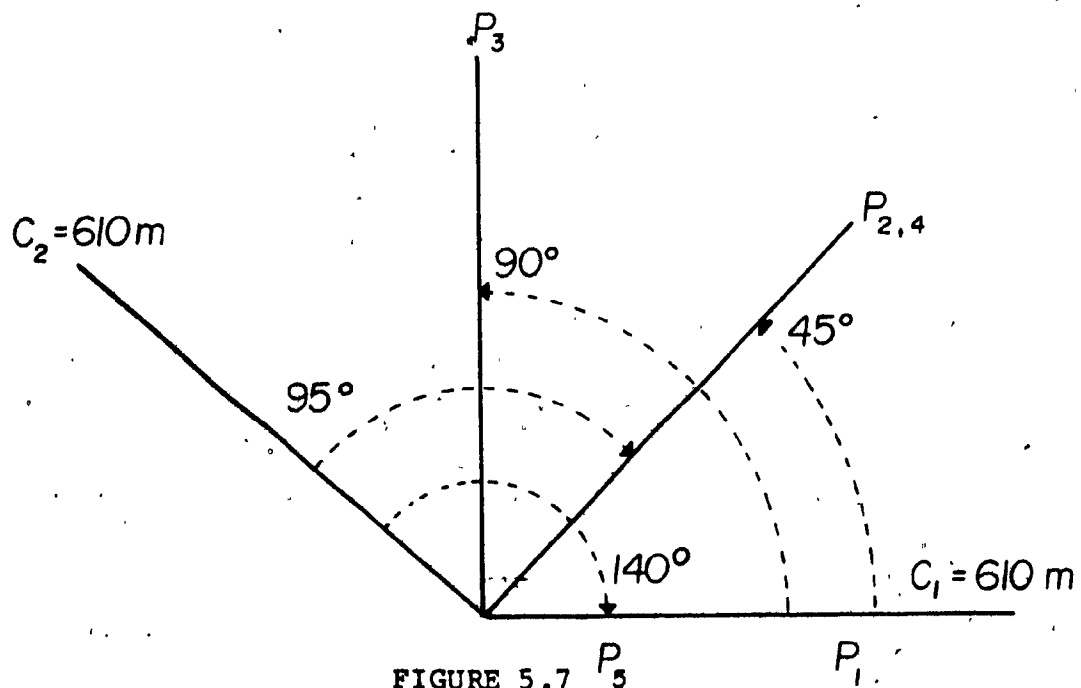


FIGURE 5.7

Probe directions in the frequency-scanning method

Table 5.2. The technique employed is described in reference [46] and a digital program was used for this purpose. Because the angle between P and C is greater than 90 degrees ( $140^\circ$ ), the resulting effect is a negative mutual coupling. This is observed in figure 5.8, where the two ground impedance curves at 140 degrees are shown, curve Z represents the measured values, and curve  $Z_g$  is obtained by taking the ground impedance measured and subtracting the calculated mutual coupling effect. From figure 5.8,  $Z_g$  was found to be  $137 \angle 16^\circ$  (m  $\Omega$ ).

b) Example with  $\theta < 90$  degrees.

Direction  $P_1$  has an angle of zero degrees with respect to  $C_1$ , and so a positive mutual effect is expected. As in the previous example, figure 5.9 displays both the curve with the measured values (Z) and the one with the final ground impedance magnitudes ( $Z_g$ ), without mutual effect. From the former curve, a value of Z cannot be established because of the increasing mutual effect, but after removing it, the latter curve shows a flat portion at approximately 127 m $\Omega$ .

#### 5.4.4 Final results

In the same way as in the two previous examples the ground impedance  $Z_g$  for the other three directions was

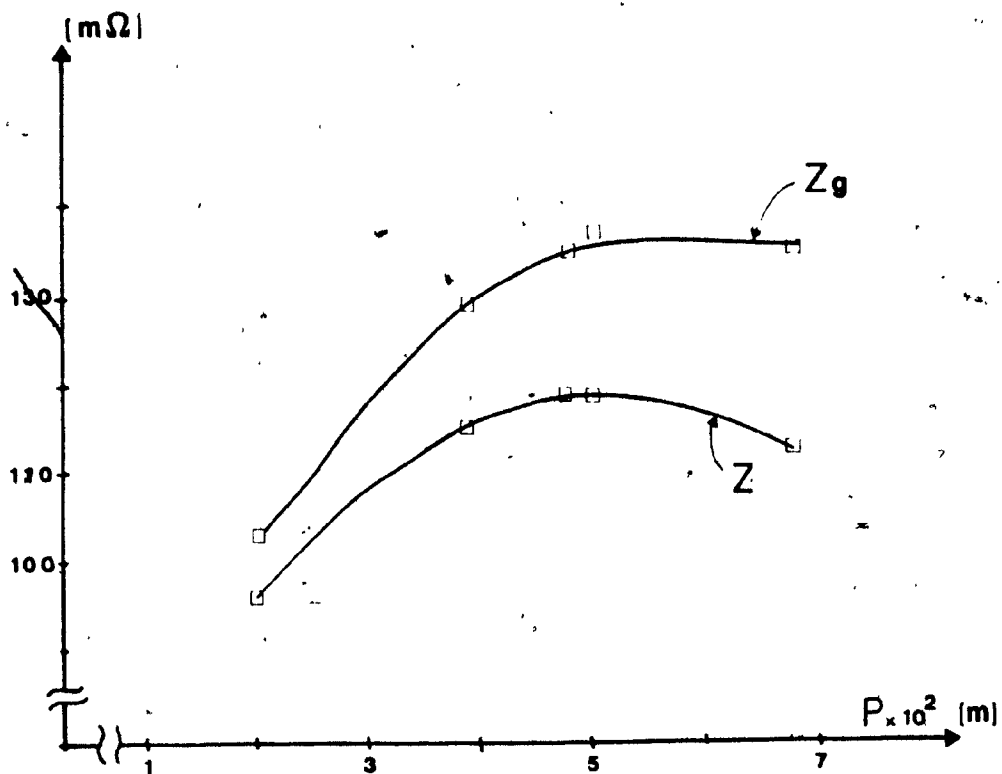


FIGURE 5.8

Ground impedance vs. distance P for direction  $P_5$

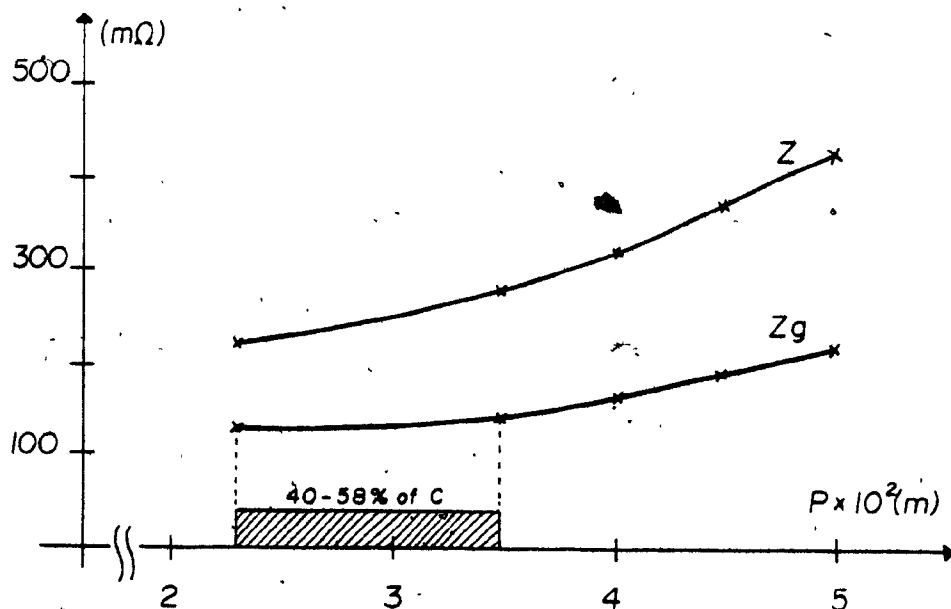


FIGURE 5.9

Ground impedance vs. distance P for direction  $P_1$

established. The results are shown in table 5.3.

TABLE 5.3

	$Z(m\Omega)$	$Z_g(m\Omega)$
0	--	127 <u>/35</u>
45	173 <u>/25</u>	135 <u>/4</u>
90	128 <u>/15</u>	128 <u>/15</u>
95	127 <u>/18</u>	130 <u>/18</u>
140	121 <u>/15</u>	137 <u>/16</u>

From table 5.3 above we can plot the values of  $Z$  and  $Z_g$  against the angle  $\theta$  between the auxiliary probes  $P$  and  $C$ , as shown in figure 5.10. In the curve for the ground impedance measured values ( $Z$ ), we clearly observe how these values are affected by mutual coupling as the angle  $\theta$  between  $P$  and  $C$  varies. This last curve is very similar to the one analytically calculated in figure 2 of reference [46] and reproduced here in figure 5.11.

On the other hand, the curve for the ground impedance  $Z_g$  gives similar values at every angle  $\theta$ , suggesting a successful application of the technique to remove the mutual coupling effects. Finally, let's perform some simple statistical operations on the values of  $Z_g$  in table 5.3:

$$\text{Average of } Z_g \text{ at } 60 \text{ Hz} = 131.6 \text{ } \underline{/17} \text{ (m } \Omega \text{ )}$$



Standard Deviation (s) = 4.61 (m  $\Omega$  )

Coefficient of variation = 3.5%

From the results presented in this chapter it is concluded that low current testing gives accurate results (comparable to a more expensive and less safe high current injection technique) as shown below:

$$Z_g(\text{with HC}) = 124 \underline{15} \quad (\text{m } \Omega)$$

$$Z_g(\text{with LC}) = 132 \underline{17} \quad (\text{m } \Omega)$$

A difference of only 5% is observed if we take the HC value as reference.

### 5.5 Interpolation of the Final Ground Impedance

#### Without Calculating Mutual Coupling Effects.

Another set of grounding tests was performed at a substation called Becancour, also part of Hydro-Quebec's electric power network. As was the case at Yamaska substation, the primary objective was to compare different techniques for measuring low ground impedances, particularly compare high and low current injection methods. The high current testing (similar to the one described in the above sections) yielded a ground impedance of 55 m- $\Omega$ . One of the low current methods employed was the one reported by Zupa-Laidig [29] also described in Chapter 4, section 4.2.

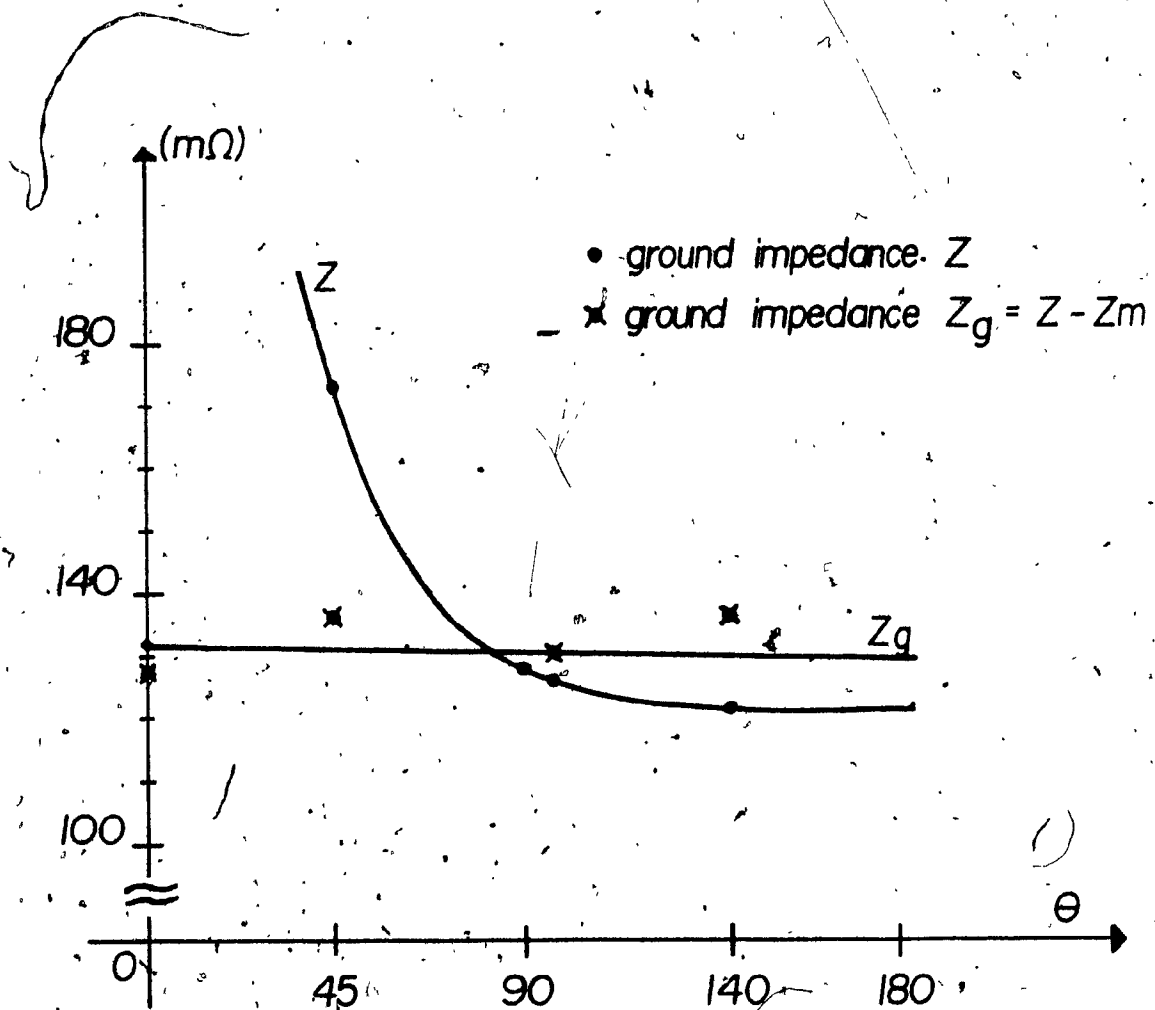


FIGURE 5.10

Ground impedance at different angles  
between P and C auxiliary leads

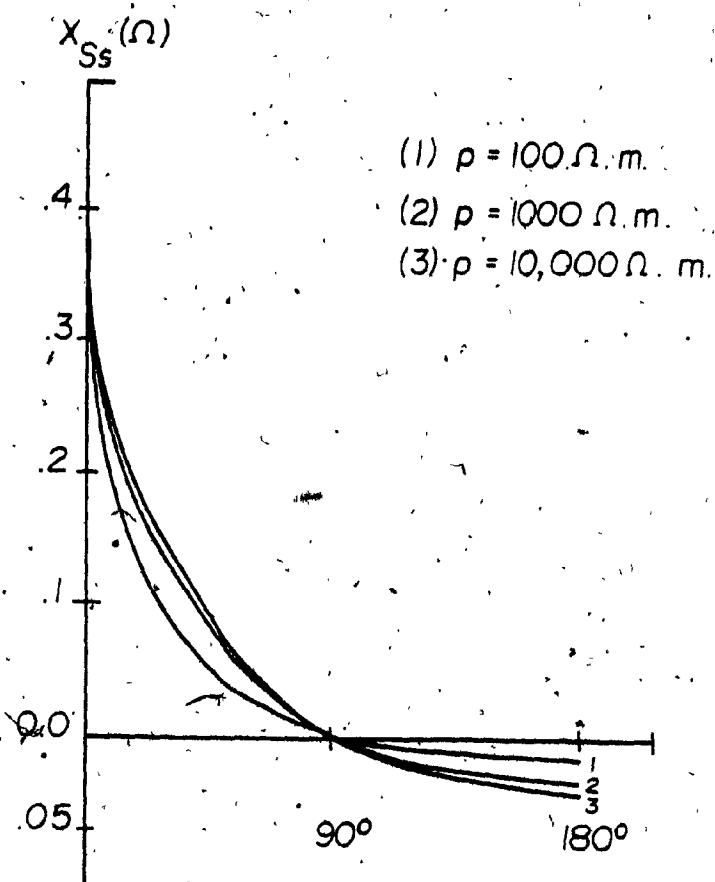


FIGURE 5.11

Analytically determined mutual reactance ( $X_{Ss}$ )  
 against angle between P and C  
 (from reference [46])

For the tests at Becancour, a frequency of 64 Hz was used, with the current injected at 100 mA. The phase angle was not measured, and so the mutual effects cannot be accounted for accurately. Nevertheless, it was possible to take several measurements at different angles between auxiliary electrodes P and C. Once the curve ground impedance vs. angle,  $\theta$  was obtained, two analyses were done:

a) Smoothing of the curve by means of a computer subroutine called ICSMOU which is part of the International Mathematical and Statistical Library [25]. This subroutine was designed to smooth a data set which is mildly contaminated with isolated errors.

b) Interpolation of the value at 90 degrees (since we know that at this angle the mutual effects are minimum), again with the use of another IMSL routine called IQHSCU which computes the coefficients for a set of cubic polynomials (quasi-Hermite spline) to be used to interpolate a set of points from a single-valued function. The purpose of a quasi-Hermite spline is to approximate a curve drawn manually.

The final curve is shown in figure 5.12 and the interpolated value is 56 m $\Omega$ . This result is interesting since it shows an alternative way of getting around the mutual coupling between auxiliary leads provided it is possible during field testing to take measurements in

different directions. On the other hand, since  $56 \text{ m}\Omega$  is almost equal to the value obtained at HC testing, this result shows that very low ground impedances can be measured with very low test currents, with values comparable to a high current test.

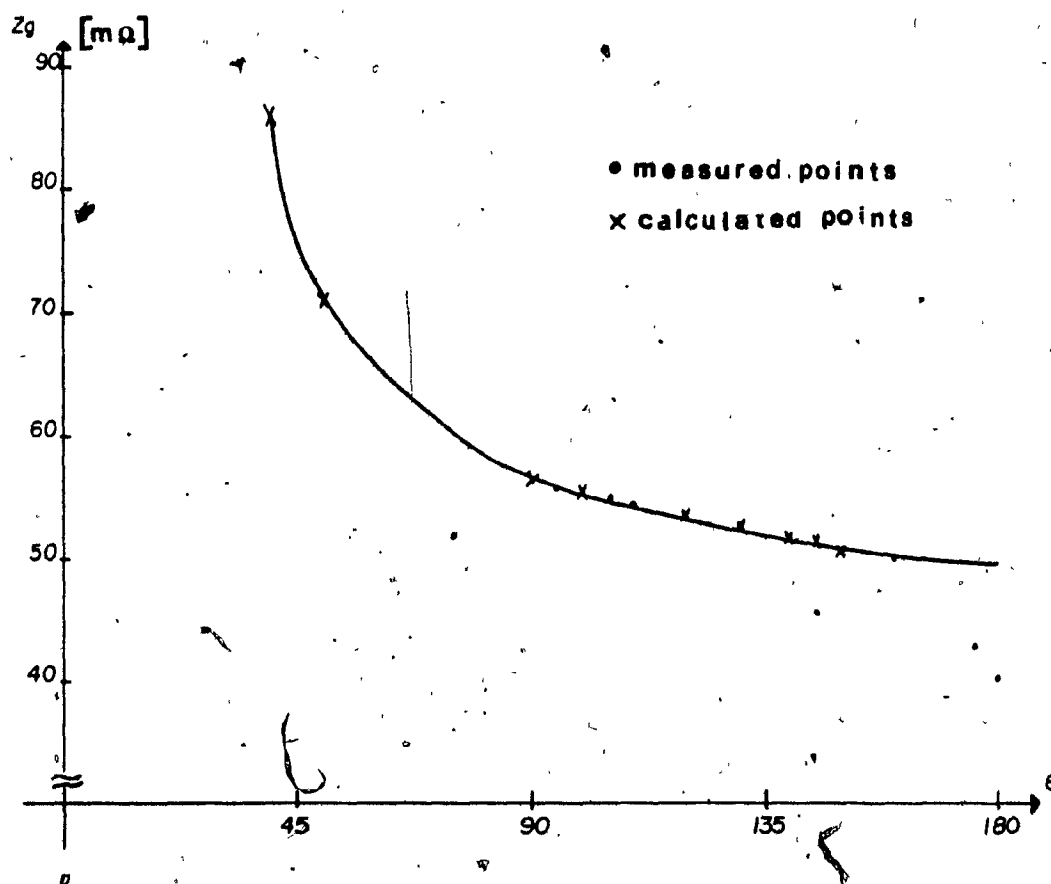


FIGURE 5.12  
 Ground impedance against  
 angle between P and C  
 after applying smoothing subroutine

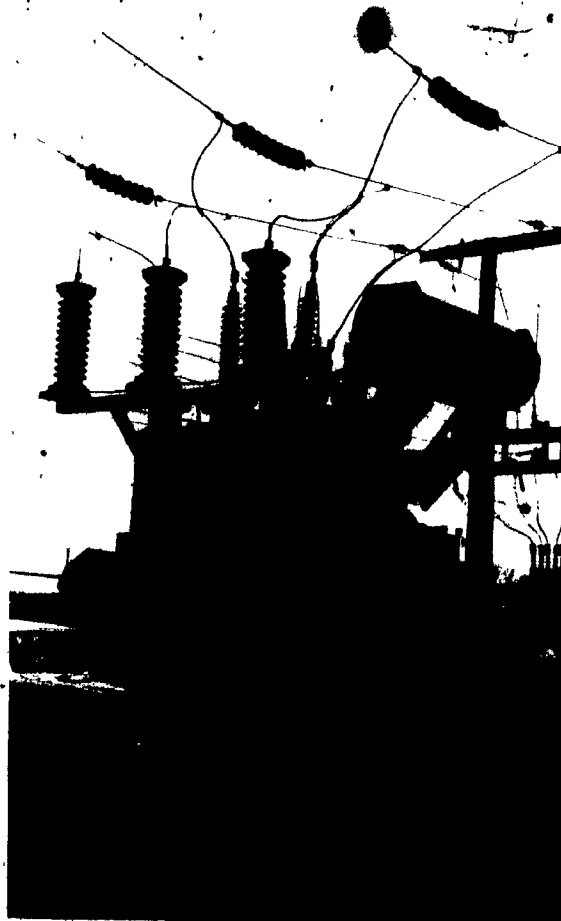


FIGURE 5.13

Delta-star 120-25 kV three-phase transformer  
used to inject fault current into the ground  
in the High Current injection method.

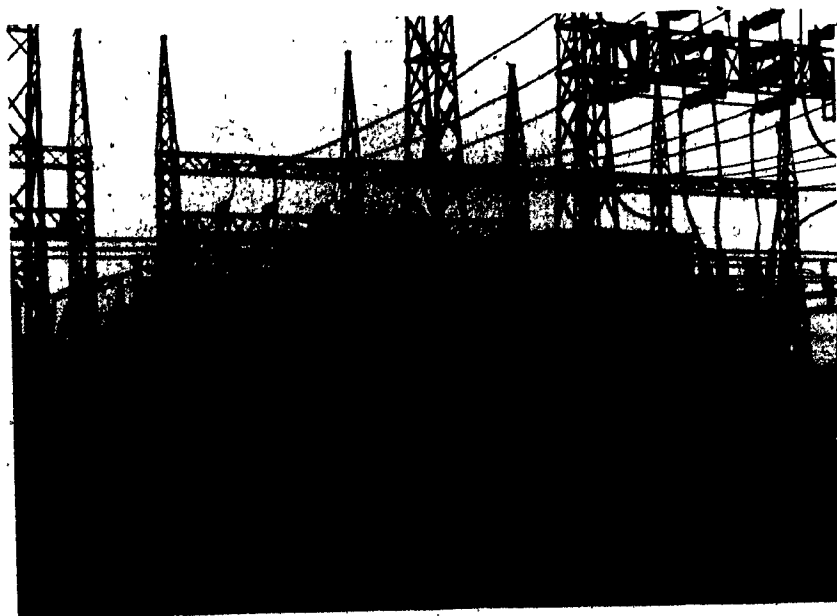


FIGURE 5.14

Truck inside Becancour substation where all  
field measurements were procured.





FIGURE 5.15

Test Bench: Where all signals from current  
and potential probes are collected.

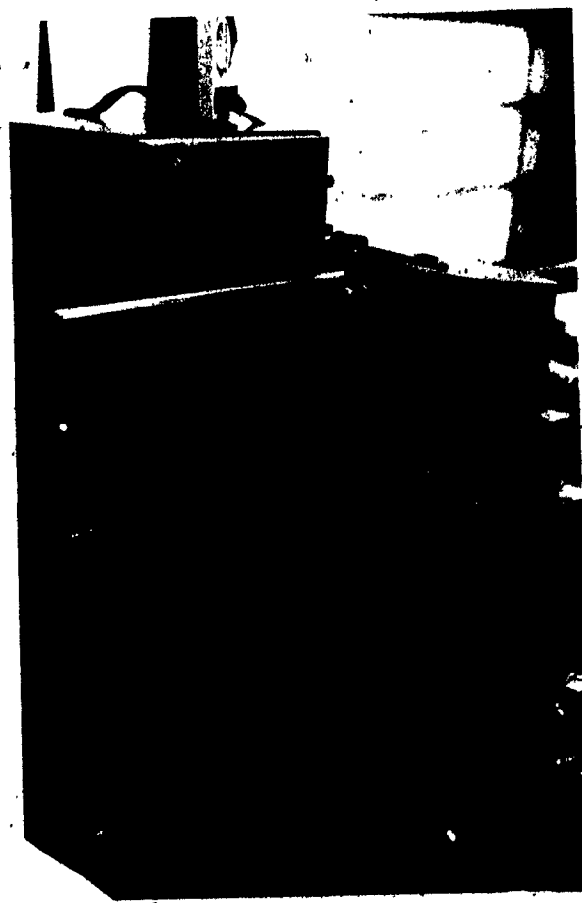


FIGURE 5.16

Spectrum Analyzer, filter, and oscillator, utilized  
in the Low Current injection methods.

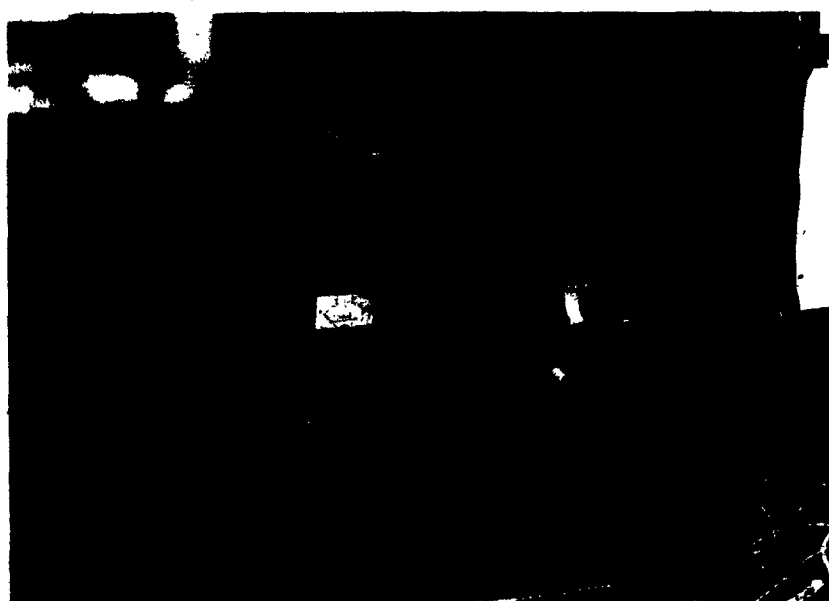


FIGURE 5.17

Ammeter and power source for the low current  
injection methods.

## CHAPTER 6

### MUTUAL COUPLING EFFECTS BETWEEN AUXILIARY CURRENT AND POTENTIAL LEADS

#### 5.1 General Background.

The mutual impedances of earth-return conductors are of relevance in studies of inductive interference in communication circuits from nearby power lines or electrified railways, in connection with propagation along extensive grounded structures, and as a first step in the calculation of voltages in power lines or communication circuits due to lightning surges or other transients. Within the framework of the present thesis, the importance of the mutual impedance between auxiliary current and potential probes was illustrated in Chapter 5, when attempting to measure very low ground impedances, in the order of  $1.0 \Omega$  or less. This mutual coupling effect is defined as the voltage induced in the potential probe by virtue of one ampere of circulating current in the current probe. This induced voltage is vectorially additive to the desired measured voltage and produces a measurement error.

Ever since the first low current methods for ground impedance testing were reported in the literature, the need to account for the mutual coupling was mentioned, since some

of the traditional ways to calculate mutual impedances prove inaccurate for this type of application. The following section elaborates on this subject.

#### 6.1.1 Mutual Impedance Between Two Conductors in the Scope of Low Ground Impedance Measurements.

The problem relies on the fact that equations for resolving mutual impedances traditionally consider two infinite parallel wires, and a corresponding expression is then derived. For example, in the case of two wires, one longer than the other, the mutual impedance calculated with Carson's equations [5] would give the mutual coupling up to the length of the shorter wire only. The following example will illustrate how formulae for infinite conductors can sometimes give erroneous results when measuring low ground impedances.

During field measurements at Becancour substation, and with the instrument described in Section 4.3, the following reading was taken:

$X = \text{inductive reactance at } 146 \text{ Hz} = 691 \text{ m}\Omega$

with the following set-up:

$C = 2\ 255 \text{ m}$

$P = 1\ 341 \text{ m}$

$$y = 7.520 \text{ m}$$

$$\rho = 25 \text{ } \Omega\text{-m}$$

The mutual effect was removed with three different expressions:

1) The following simplified equation, which gives the mutual inductance in henrys.

$$L_m = 2P(\ln(2P/y) - 1) \times 10^{-7}$$

2) Carsons's equations for mutual impedance.

3) Equations developed in [45] for finite conductors.

The final mutual inductive reactance for each of the three cases is:

$$1) X_g = X - X_m = 691 - 1196 = -505 \text{ m}\Omega$$

$$2) X_g = 691 - 880 = -189 \text{ m}\Omega$$

$$3) X_g = 691 - 496 = 195 \text{ m}\Omega$$

Since we are dealing with an impedance of less than  $0.5 \text{ } \Omega$ , the formulae for infinite conductors are not accurate enough, only the equation for finite conductors gives a logical result.

What is needed, then, are expressions including the so called "end effects", or in other words, expressions dealing with finite conductors. Additionally, as illustrated in the previous chapter, the auxiliary leads P and C do not always run parallel to each other, but may form an angle between

them. Carson's or similar equations are not suitable to calculate the mutual impedance for these cases.

#### 6.1.2 Two Conductors Lying on the Surface of the Ground.

The first results in this direction were reported by Velazquez, et.al. [45], for two conductors lying on the earth's surface. This is a typical arrangement for ground impedance measurements with low current methods, where both the current and potential probes are laid out in the field by means of temporary field cables on the soil surface. The expressions developed in that paper originate from the general equation proposed first by Foster [17]:

$$Z_m = \int_0^C \int_0^P \left[ \frac{\rho}{2\pi} \frac{d^2}{dP dC} \left( \frac{1}{r} \right) + \frac{i\omega \cos\theta}{r} \left\{ \frac{2}{(\gamma r)^2} \left[ 1 - (1 + \gamma r) e^{-\gamma r} \right] \right\} \right] dP dC \quad (5.1)$$

This formula gives the mutual impedance between two insulated wires of length P and C, of negligible diameter, lying on the surface of the earth, and grounded at their end-points. This mutual effect is the result of the axial

electric intensity in one of the wires due to the varying magnetic field of unit current in the other wire and its accompanying distribution of ground current.

The terms in this equation are:

$\rho$  = soil resistivity in ohm-m (from a two layer model, an equivalent resistivity can be determined from the curves in [43], Chapter 2).

$r$  = distance between two infinitesimal elements

$dP$  and  $dC$  of conductors  $P$  and  $C$ .

$\omega$  = angular frequency in rad/s =  $2\pi f$  (where  $f$  is the frequency in Hz).

$\theta$  = angle between conductors  $P$  and  $C$ .

$\gamma$  = propagation constant for plane electromagnetic waves  
 $= \sqrt{i \omega \nu / \rho}$

This equation was reduced to the following expression, as shown in [46] and [47]:

$$Z_m = R(P)(C) + \frac{i \omega \nu \cos \theta}{4\pi} \left[ M - \frac{2}{3} \gamma PC \right] \quad (5.2)$$

where:

$$R(P)(C) = \frac{\rho}{2\pi} \int_0^C \int_0^P \frac{d^2}{dPdC} \left( \frac{1}{r} \right) dPdC \quad (5.3)$$

$R_{pc}$  = mutual dc resistance



$$M = \int_0^C \int_0^P \frac{dP}{r} dC$$

(5.4)

is called the Neumann integral.

Subsequently, expressions are found for establishing the mutual impedance of two conductors on the earth's surface for two cases, representing typical field measurement arrangements:

- 1) Parallel conductors
- 2) Angled conductors starting at the same point.

These equations were tested and calibrated in the present work.

The purpose of this chapter is to extend this work for the case when one of the conductors is lying on the surface of the earth, but the other one is at any height, either in the same direction as the first one, or with an angle between their directions. This case usually arises when using high current methods, in which a HV transmission line conductor is used to inject the test current. In some other cases, telephone pairs or distribution lines are used, particularly with urban and suburban substations, when it is difficult to lay out cables on the ground.

## 6.2 Analytical Development.

Foster, in a later paper [18], shows that the same equation (5.2) can be applied for finite conductors grounded at both ends and above the ground. That is, all terms remain the same as with the case for conductors lying on the earth's surface, except the Neumann integral is to be solved accordingly, for each particular case. Hence, our problem has been restricted to finding the solution to this integral, which is done in the next sections.

### 6.2.1 Basic Assumptions.

In arriving at equation (5.2) and in solving the Neumann integral, the following assumptions were made, and remain the same during this development:

- 1) The earth is of negligible capacitivity, and of inductivity equal to that of free space.
- 2) For low frequencies, it is ordinarily permissible to neglect attenuation effects along the two wires, and in doing so, radial displacement currents are disregarded.
- 3) On a three dimensional space, the angle between two directed lines can be different from an angle between two coplanar lines. But for the two cases studied in this Chapter, it can be shown from solid geometry equations [11], that the angle is the same as in the case of two conductors on the earth's surface.

4) As pointed out in [46] and treated in more detail in [47],  $R_{pc}$  represents the mutual dc resistance between the earth electrodes at the end of the two conductors. This term does not influence the value of  $Z_m$  if the fall-of-potential method is followed carefully, and furthermore, if during the measurement itself the cables are well insulated and properly connected to the measuring instrument.

#### 6.2.2 Solution to the Neumann Integral.

The Neumann integral is solved for two cases, representing common set-ups for the potential and current auxiliary leads in ground impedance measurements:

- a) Skew conductors-Parallel directions (Figure 6.1)
- b) Skew conductors-Angle between their directions (Figure 6.2).

##### a) Parallel Directions.

A solution is desired in terms of quantities usually known or easily determined during fields measurements:

Length to the potential probe =  $P$

Length to the current probe =  $C$

Horizontal distance between both conductors =  $y$

Height of one of the conductors =  $z$

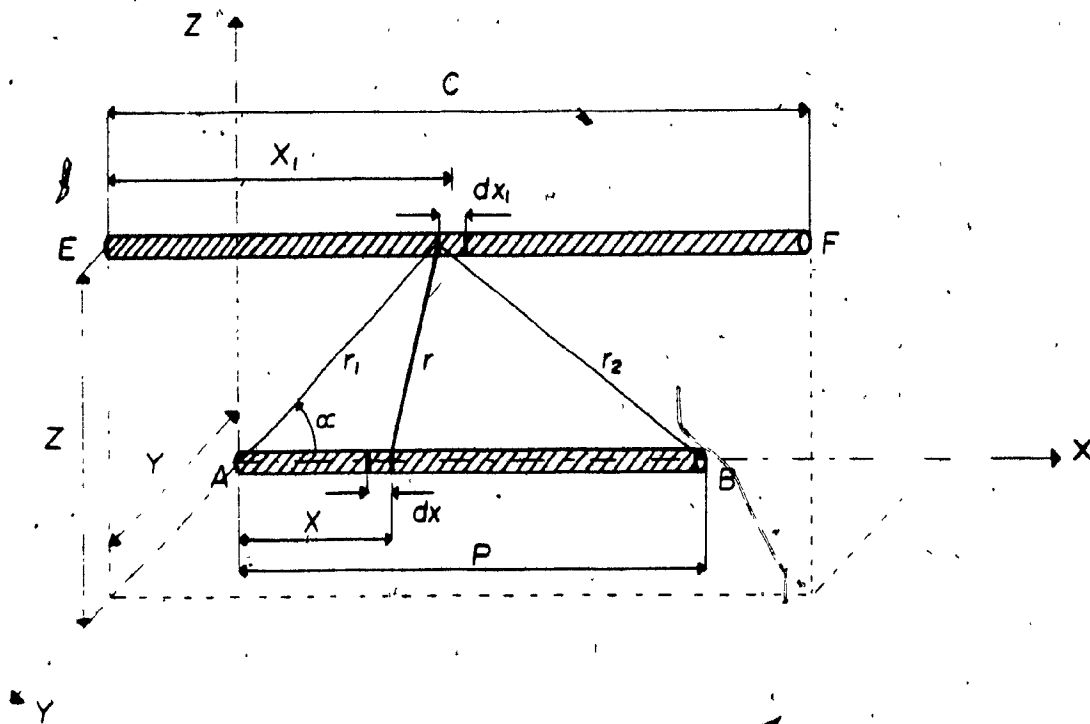


FIGURE 6.1

Conductor arrangement for parallel directions

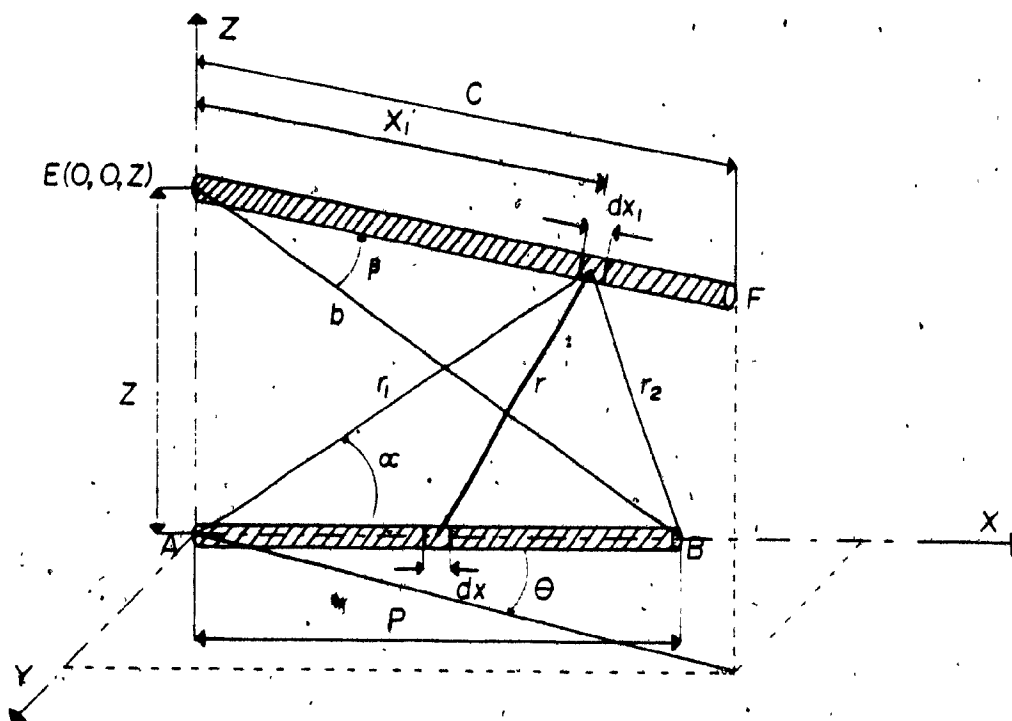


FIGURE 6.2

Conductor arrangement for angle between directions

Referring to Figure 5.1, the following is noted:

A (0, 0, 0) and B (P, 0, 0)

(that is, conductor P is placed on the x-axis, and the x-y plane represents the earth's surface).

dx (x, 0, 0)

dx<sub>1</sub> (x, y, z)

Also

$$r_1 = \sqrt{x_1^2 + y^2 + z^2}$$

$$r_2 = \sqrt{(x_1 - P)^2 + y^2 + z^2}$$

$\alpha$  = angle between line segments  $r_1$  and P

and

$$r^2 = r_1^2 + x^2 - 2r_1 x \cos \alpha$$

Substituting this last expression in the Neumann integral, eq. (5.4):

$$M = \int_E^F \int_A^B \left( \frac{dx}{\sqrt{r_1^2 + x^2 - 2r_1 x \cos \alpha}} \right) dx_1$$

The following integral is solved first:

$$\int_0^P \frac{dx}{\sqrt{r_1^2 - 2r_1 \cos \alpha x + x^2}}$$

The solution to this integral is [3]:

$$\int \frac{dx}{\sqrt{ax^2 + bx + c}} = \frac{1}{\sqrt{a}} \ln \left( 2\sqrt{a} \sqrt{ax^2 + bx + c} + 2ax + b \right)$$

where:

$$a = 1$$

$$b = -2r_1 \cos \alpha$$

$$c = r_1^2$$

Then:

$$\int_0^P \frac{dx}{\sqrt{x^2 - 2r_1 \cos \alpha x + r_1^2}} =$$

$$= \ln \left[ 2 \sqrt{x^2 - 2r_1 \cos \alpha x + r_1^2} + 2x - 2r_1 \cos \alpha \right]_0^P$$

After substitution of the limits of integration:

$$\int_A^B \frac{dx}{r} = \ln \left( \frac{P - r_1 \cos \alpha + \sqrt{P^2 - 2Pr_1 \cos \alpha + r_1^2}}{r_1 (1 - \cos \alpha)} \right)$$

(6.5)

The next step is to solve the following integral:

$$\int_E^F \left( \int_A^B \frac{dx}{r} \right) dx_1 =$$

$$= \int_0^C \text{Ln} \left( \frac{P - r_1 \cos \alpha + \sqrt{P^2 - 2Pr_1 \cos \alpha + r_1^2}}{r_1 (1 - \cos \alpha)} \right) dx_1$$

Noting from Figure 5.1 the following relationships:

$$r_1 \cos \alpha = x_1$$

$$r_1 = \sqrt{x_1^2 + y^2 + z^2}$$

And making the above substitutions:

$$M = \int_0^C \text{Ln} \left( \frac{P - x_1 + \sqrt{P^2 - 2Px_1 + x_1^2 + y^2 + z^2}}{\sqrt{x_1^2 + y^2 + z^2} + x_1} \right) dx_1$$

Breaking down the above expression into two integrals:

$$M = M_1 + M_2$$

where:

$$M_1 = \int_0^C \text{Ln} \left( P - x_1 + \sqrt{P^2 - 2Px_1 + x_1^2 + y^2 + z^2} \right) dx_1 \quad (5.5)$$

$$M_2 = - \int_0^C \text{Ln} \left( -x_1 + \sqrt{x_1^2 + y^2 + z^2} \right) dx_1 \quad (5.7)$$

Solving  $M_2$  first, with the following change of variable:

$$u = -x_1$$

$$x_1 = -u$$

$$dx_1 = -du$$

$$M_2 = \int_0^{-C} \ln \left( u + \sqrt{u^2 + y^2 + z^2} \right) du$$

The solution to this integral is, from [3]:

$$M_2 = u \times \ln \left( u + \sqrt{u^2 + y^2 + z^2} \right) - \sqrt{u^2 + y^2 + z^2} \Big|_0^{-C}$$

$$M_2 = (-C) \ln \left( -C + \sqrt{C^2 + y^2 + z^2} \right) + \\ - \sqrt{C^2 + y^2 + z^2} + \sqrt{y^2 + z^2}$$

Expression (5.6) is now solved, with the following change of variables:

$$u = P - x_1$$

$$x_1 = P - u$$

$$dx_1 = -du$$

$$M_1 = - \int_P^{P-C} \ln \left\{ u + \sqrt{u^2 + y^2 + z^2} \right\} du$$

$$= (C-P) \ln \left\{ P-C + \sqrt{(P-C)^2 + y^2 + z^2} \right\} + \sqrt{(P-C)^2 + y^2 + z^2} + \\ + (P) \ln \left\{ P + \sqrt{P^2 + y^2 + z^2} \right\} - \sqrt{P^2 + y^2 + z^2}$$

Finally:



$$M = M_1 + M_2$$

$$\begin{aligned}
 M = & (C) \ln \left\{ P-C + \sqrt{(P-C)^2 + y^2 + z^2} \right\} + \\
 & -(P) \ln \left\{ P-C + \sqrt{(P-C)^2 + y^2 + z^2} \right\} + \\
 & -(C) \ln \left\{ -C + \sqrt{C^2 + y^2 + z^2} \right\} + (P) \ln \left\{ P + \sqrt{P^2 + y^2 + z^2} \right\} \\
 & - \sqrt{P^2 + y^2 + z^2} + \sqrt{y^2 + z^2} - \sqrt{C^2 + y^2 + z^2} + \\
 & + \sqrt{(P-C)^2 + y^2 + z^2}
 \end{aligned}$$

Rearranging terms and after some algebraic manipulations to homogenize the presentation:

$$\begin{aligned}
 M = & (C) \ln \left\{ \frac{\sqrt{C^2 + y^2 + z^2} + C}{\sqrt{(P-C)^2 + y^2 + z^2} + (C-P)} \right\} + \\
 & + (P) \ln \left\{ \frac{\sqrt{P^2 + y^2 + z^2} + P}{\sqrt{(P-C)^2 + y^2 + z^2} + (P-C)} \right\} + \\
 & + \sqrt{(P-C)^2 + y^2 + z^2} - \sqrt{P^2 + y^2 + z^2} - \sqrt{C^2 + y^2 + z^2} + \\
 & + \sqrt{y^2 + z^2}
 \end{aligned}$$

(6.8)

This solution to the Neumann integral, used in the following equation, will give the mutual impedance of two skew conductors with parallel directions:

$$Z_m = j \left( \frac{\omega \mu}{4\pi} \right) \left[ M - \frac{2}{3} \gamma PC \right] \Omega$$

b) Angle between their Directions. (See figure 6.2)

Again, it is desired to find a solution in terms of known or easily determined quantities: P, C, z, and in this case  $\theta$ . Equation (6.5) already shows the solution to one of the integrals and is repeated here:

$$\int_0^P \frac{dx}{\sqrt{r_1^2 - 2r_1 \cos \alpha x + x^2}} =$$

$$= \text{Ln} \left\{ \frac{P - r_1 \cos \alpha + \sqrt{r_1^2 + P^2 - 2Pr_1 \cos \alpha}}{r_1 (1 - \cos \alpha)} \right\}$$

From Figure 6.2, the following relationships apply:

$$r_1 = \sqrt{x_1^2 + z^2}$$

$$r_2 = \sqrt{x_1^2 + b^2 - 2bx_1 \cos \beta}$$

$$r_1 \cos \alpha = x_1 \cos \theta$$

$$b \cos \beta = P \cos \theta$$

The following integral, then, is to be solved:

$$M = \int_0^C \ln \left\{ \frac{P - r_1 \cos \alpha + r_2}{r_1 - r_1 \cos \alpha} \right\} dx_1$$

Making the substitutions outlined above:

$$M = \int_0^C \ln \left\{ \frac{P - x_1 \cos \theta + \sqrt{x_1^2 + b^2 - 2bx_1 \cos \beta}}{\sqrt{x_1^2 + z^2} - x_1 \cos \theta} \right\} dx_1$$

The above integral is split in two:

$$M = M_1 - M_2$$

where:

$$M_1 = \int_0^C \ln \left\{ P - x_1 \cos \theta + \sqrt{(x_1 - b \cos \beta)^2 + (b \sin \beta)^2} \right\} dx_1$$

Note that:

$$x_1^2 + b^2 - 2bx_1 \cos \beta = (x_1 - b \cos \beta)^2 + (b \sin \beta)^2$$

And:

$$M_2 = \int_0^C \ln \left\{ -x_1 \cos \theta + \sqrt{x_1^2 + z^2} \right\} dx_1$$

The solution to the above integrals is of the form [31]:

$$\begin{aligned}
& \int \text{Ln} \left( m + nu + \sqrt{u^2 + k^2} \right) du = \\
& = \left( u - \frac{mn}{1-n^2} \right) \text{Ln} \left( m + nu + \sqrt{u^2 + k^2} \right) + \\
& + \left( \frac{m}{1-n^2} \right) \text{Ln} \left\{ u + \sqrt{u^2 + k^2} \right\} - u + \\
& + \frac{2 \sqrt{(1-n^2) k^2 - m^2}}{1-n^2} \tan^{-1} \left\{ \frac{(1+n) (u + \sqrt{u^2 + k^2}) + m}{\sqrt{(1-n^2) k^2 - m^2}} \right\}
\end{aligned}$$

(6.9)

Starting with  $M_1$ , the following change of variables is made:

$$u = x_1 - b \cos \beta$$

$$du = dx_1$$

Then:

$$M_1 = \int_{-b \cos \beta}^{C - b \cos \beta} \text{Ln} \left\{ P - b \cos \beta \cos \theta - u \cos \theta + \sqrt{u^2 + (b \sin \beta)^2} \right\} du$$

Where:

$$m = P - b \cos \beta \cos \theta$$

$$n = -\cos \theta$$

$$k = b \sin \beta$$

Making the necessary substitutions in the solution to the integral and replacing the upper and lower limits:

$$M_1 = \left[ \frac{C - b \cos \beta - (P - b \cos \beta \cos \theta)(-\cos \theta)}{1 - \cos^2 \theta} \right] \times$$

$$\left\{ \ln \left\{ P - b \cos \beta \cos \theta - (C - b \cos \beta) \cos \theta + \right. \right.$$

$$\left. + \sqrt{(C - b \cos \beta)^2 + (b \sin \beta)^2} \right\} +$$

$$+ \left( \frac{P - b \cos \beta \cos \theta}{1 - \cos^2 \theta} \right) \ln \left\{ C - b \cos \beta + \sqrt{(C - b \cos \beta)^2 + (b \sin \beta)^2} \right\} +$$

$$- (C - b \cos \beta) +$$

$$\frac{2 \sqrt{(1 - \cos^2 \theta)(b \sin \beta)^2 - (P - b \cos \beta \cos \theta)^2}}{1 - \cos^2 \theta} \times$$

$$\tan^{-1} \left\{ \frac{(1 - \cos \theta)(C - b \cos \beta + \sqrt{(C - b \cos \beta)^2 + (b \sin \beta)^2} + P - b \cos \beta \cos \theta)}{\sqrt{(1 - \cos^2 \theta)(b \sin \beta)^2 - (P - b \cos \beta \cos \theta)^2}} \right\}$$

$$- \left\{ \left[ -b \cos \beta - \frac{(P - b \cos \beta \cos \theta)(-\cos \theta)}{1 - \cos^2 \theta} \right] \ln \left\{ P - b \cos \beta \cos \theta + \right. \right.$$

$$\left. - (-b \cos \beta) \cos \theta + \sqrt{(b \cos \beta)^2 + (b \sin \beta)^2} \right\} +$$

$$+ \left[ \frac{P - b \cos \beta \cos \theta}{1 - \cos^2 \theta} \right] \ln \left\{ -b \cos \beta + \sqrt{(b \cos \beta)^2 + (b \sin \beta)^2} \right\} +$$

$$+ b \cos \beta + \frac{2 \sqrt{(1 - \cos^2 \theta) (b \sin \beta)^2 - (P - b \cos \beta \cos \theta)^2}}{1 - \cos^2 \theta} \times$$

$$\tan^{-1} \left[ \frac{(1 - \cos \theta) (-b \cos \beta + \sqrt{(b \cos \beta)^2 + (b \sin \beta)^2 + P - b \cos \beta \cos \theta})}{\sqrt{(1 - \cos^2 \theta) (b \sin \beta)^2 - (P - b \cos \beta \cos \theta)^2}} \right]$$

Using the following equalities:

$$b \cos \beta = P \cos \theta$$

$$b = \sqrt{P^2 + z^2}$$

$$\tan \frac{\theta}{2} = \frac{1 - \cos \theta}{\sin \theta}$$

And after some algebra:

$$M_1 = (C) \ln \left\{ \sqrt{C^2 + P^2 - 2CP \cos \theta + z^2} + P - C \cos \theta \right\} +$$

$$+ (P) \ln \left\{ \frac{\sqrt{C^2 + P^2 - 2CP \cos \theta + z^2} + C - P \cos \theta}{\sqrt{P^2 + z^2} - P \cos \theta} \right\} - C$$

$$+ \frac{2z}{\sin \theta} \left\{ \tan^{-1} \left[ \tan \frac{\theta}{2} \left( \frac{\sqrt{C^2 + P^2 - 2CP \cos \theta + z^2} + C + P}{z} \right) \right] \right.$$

$$\left. - \tan^{-1} \left[ \tan \frac{\theta}{2} \left( \frac{\sqrt{P^2 + z^2} + P}{z} \right) \right] \right\}$$

Now let's proceed with  $M_2$ :

$$M_2 = \int_0^C \ln \left\{ -x_1 \cos \theta + \sqrt{x_1^2 + z^2} \right\} dx_1$$

Substituting in the proper solution (5.9) and with:

$$n = -\cos \theta$$

$$m = 0$$

$$k = z$$

Therefore:

$$M_2 = (x_1) \ln \left\{ -x_1 \cos \theta + \sqrt{x_1^2 + z^2} \right\} - x_1 + \\ + \frac{2 \sqrt{(1 - \cos^2 \theta) z^2}}{1 - \cos^2 \theta} \tan^{-1} \left\{ \frac{(1 - \cos \theta) (x_1 + \sqrt{x_1^2 + k^2})}{\sqrt{(1 - \cos^2 \theta) z^2}} \right\} \Bigg|_0^C$$

Substituting upper and lower limits:

$$M_2 = (C) \ln \left\{ -C \cos \theta + \sqrt{C^2 + z^2} \right\} - C + \frac{2z}{\sin \theta} \left( \tan^{-1} x \right. \\ \left. \left\{ \tan \frac{\theta}{2} \left[ \frac{\sqrt{C^2 + z^2} + C}{z} \right] \right\} - \tan^{-1} \left[ \tan \frac{\theta}{2} \right] \right)$$

And finally, after grouping terms:

$$M = M_1 - M_2$$

$$M = (C) \ln \left\{ \frac{\sqrt{C^2 + P^2 - 2CP \cos \theta + z^2} + P - C \cos \theta}{\sqrt{C^2 + z^2} - C \cos \theta} \right\} + \\ + (P) \ln \left\{ \frac{\sqrt{C^2 + P^2 - 2CP \cos \theta + z^2} + C - P \cos \theta}{\sqrt{P^2 + z^2} - P \cos \theta} \right\} + \\ + \frac{2z}{\sin \theta} \left\{ \tan^{-1} \left[ \tan \frac{\theta}{2} \left( \frac{\sqrt{C^2 + P^2 - 2CP \cos \theta + z^2} + C + P}{z} \right) \right] \right\} +$$

$$\begin{aligned}
& -\tan^{-1} \left[ \tan \frac{\theta}{2} \left( \frac{\sqrt{P^2 + z^2} + P}{z} \right) \right] + \\
& -\tan^{-1} \left[ \tan \frac{\theta}{2} \left( \frac{\sqrt{C^2 + z^2} + C}{z} \right) \right] + \tan^{-1} \left( \tan \frac{\theta}{2} \right) \Bigg\}
\end{aligned}$$

(5.10)

It is important to emphasize that the solution to the Neumann integral found in equations (5.8) and (6.10) above, represents broader expressions than the ones in [45], in the sense that one of the conductors can be at any height, and by setting this height to zero, the equations are converted to the ones for two finite conductors resting on the earth's surface.

### 6.3. Sensitivity Analysis.

Before discussing the results of these analyses, it should be pointed out that the problem of finding the mutual impedance of two grounded conductors, in this particular case one of them at any height and the other lying on the earth's surface, is a boundary value problem involving cylindrical conductors. Hence, the "method of images" can be applied [2]. This well-known method makes use of the fact that the influence of the ground on the charges and



potentials of the conductors can be equivalently replaced by the influence of the images of the conductors below the surface of the ground. Any one conductor and its image are located at equal distance, but in opposite directions from the ground surface. The potential at any point in the system can be obtained by calculating that due to the charge itself and adding to it the potential due to its images [45]. In other words, for the cases dealt with in this chapter, the solution to the Neumann integral is simply recalculated, inserting a negative height ( $-z$ ) to account for the overhead conductor's image [22].

With the expressions derived for the two cases described in Section 5.2, the behaviour of the real (resistance) and imaginary (reactance) parts against variations in the following parameters was analyzed: Soil resistivity, length of conductors, angle between the conductors, horizontal distance between the conductors, and height of the overhead conductor. Only those curves where the height of one conductor is varied will be shown, since other results from the sensitivity analysis followed very closely the one presented in [46] for two conductors resting on the ground. The main points, though, will be repeated here:

- i) At 90 degrees,  $Z_m$  is minimum, and should be the preferred conductor disposition, provided the field conditions allow

it.

ii)  $Z_m$  increases linearly with increasing lengths of P and C.

iii)  $Z_m$  tends to increase the measured value of the ground impedance in the range  $\theta$  greater than 90 degrees. For values greater than 90 degrees, the measured values are somewhat less.

iv) Horizontal separation  $y$  has minimum effect.

Figures 6.3, 6.4, and 6.5 show the effect of the height on the mutual ground impedance values. Only typical heights of telephone, distribution, and HV lines are presented. These structures are commonly used as potential and/or current auxiliary probes. The conclusions drawn from these curves are:

v) For a wide variety of soil resistivity values, the imaginary part of the mutual impedance shows a small variation with different heights, and has no bearing at all on the real part.

vi) Height is insignificant when the horizontal distance ( $y$ ) between the two conductors is varied, except at very short distances.

vii) The height has no impact with variations of the angle between the auxiliary probes. All the analysis was made for a frequency of 50 Hz.

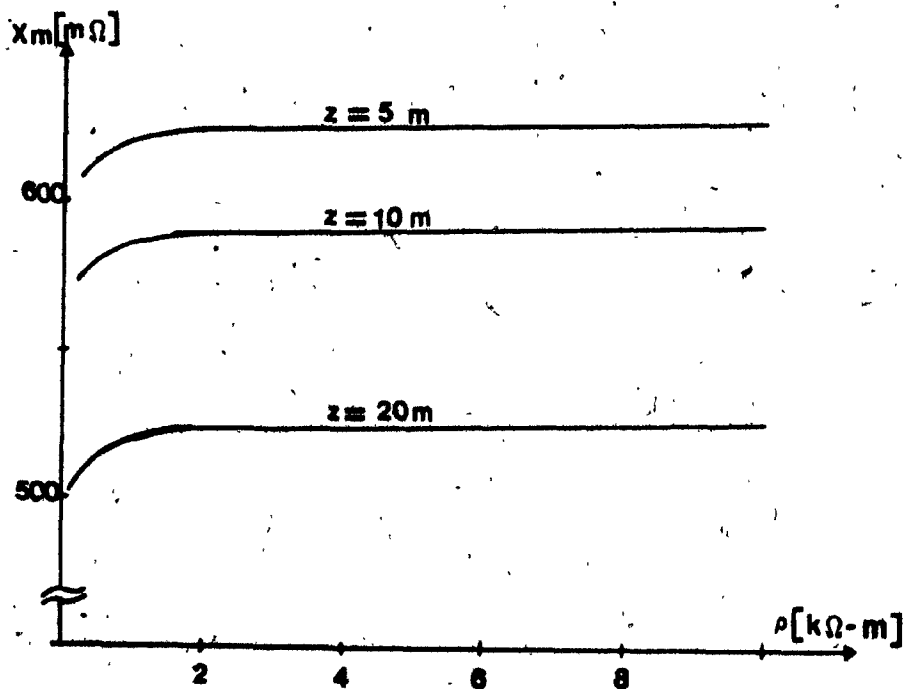
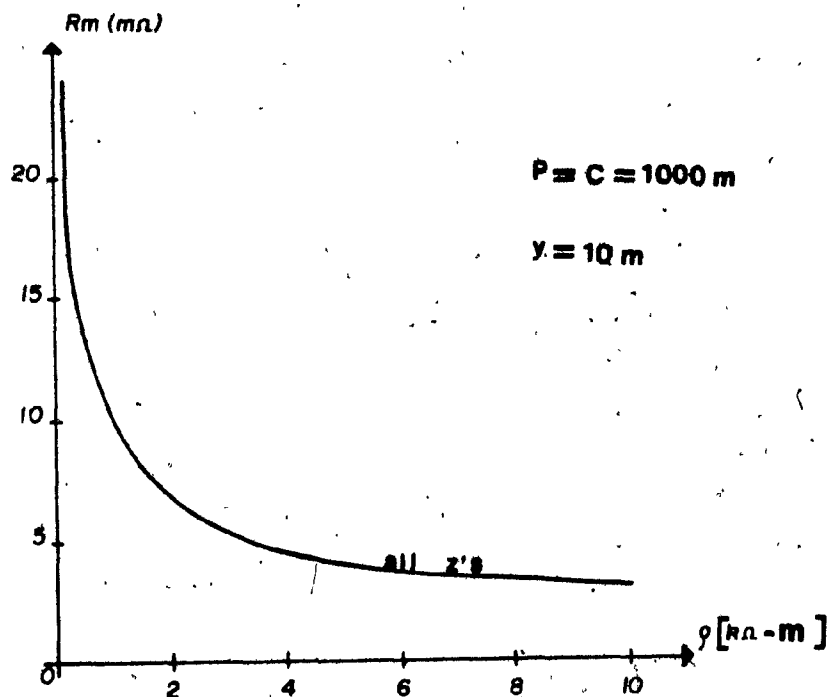


FIGURE 6.3

Effect of resistivity and height  
on the mutual impedance

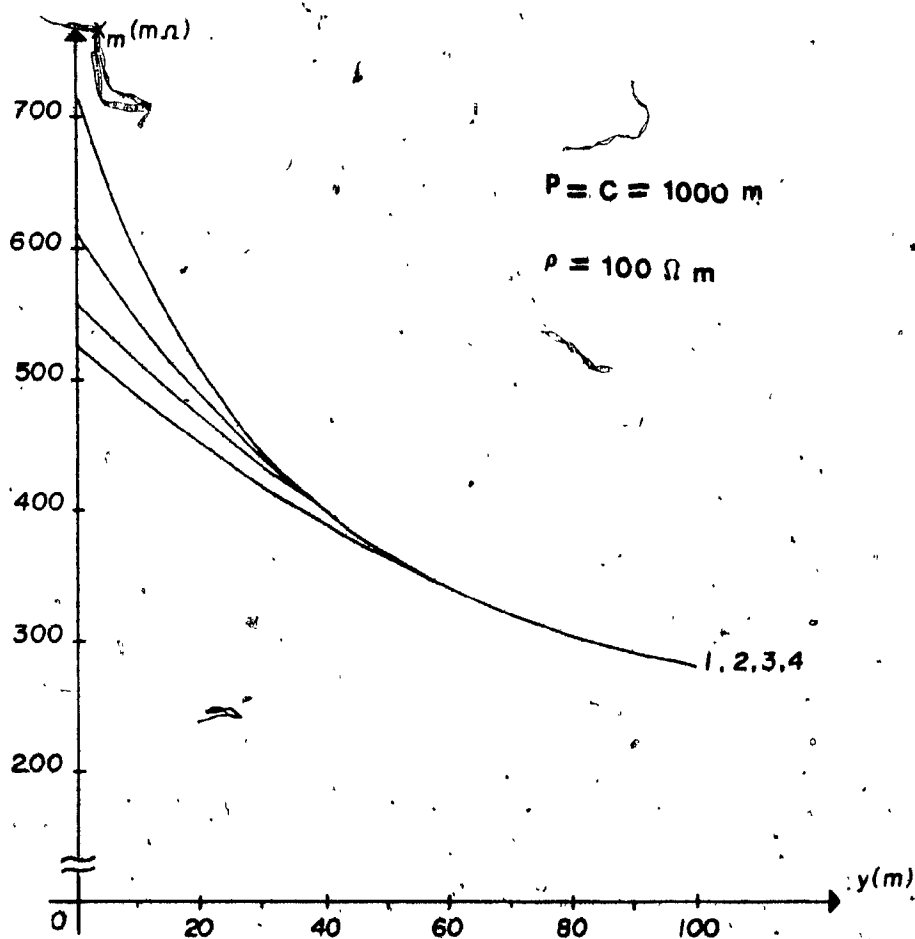
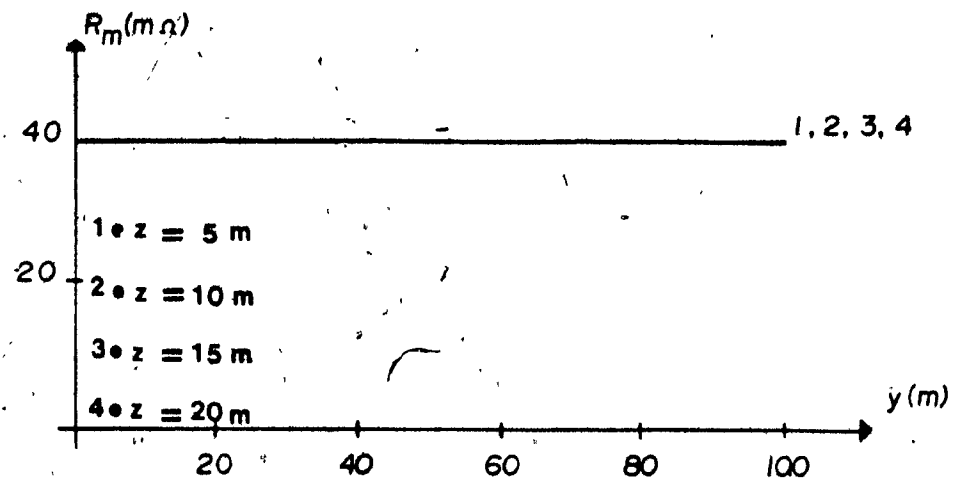
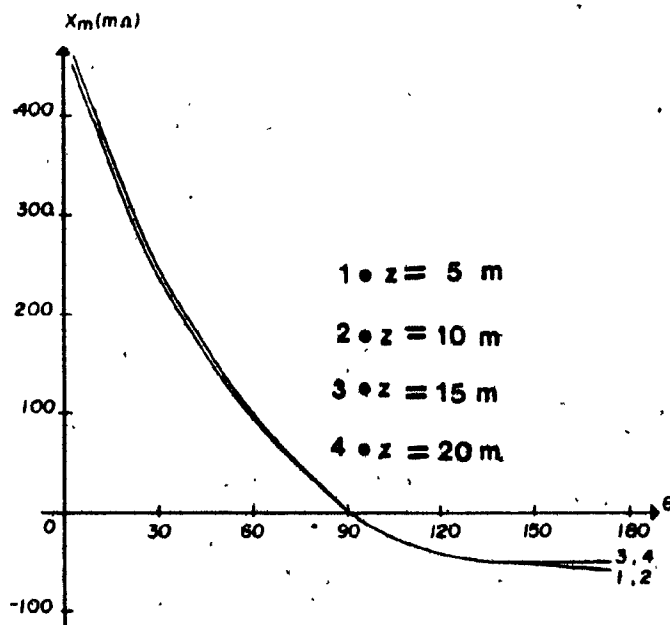
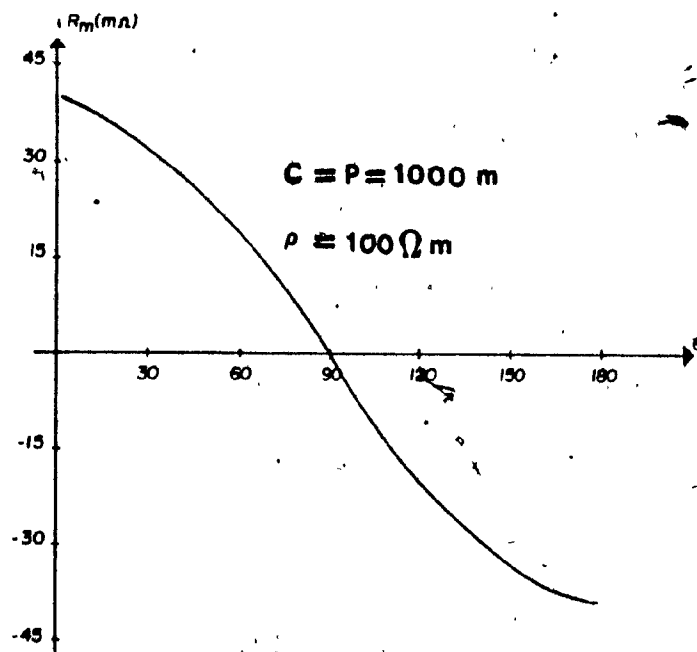


FIGURE 6.4

Effect of the height and distance between  
conductors on the mutual impedance



**FIGURE 6.5**  
Effect of the angle between conductors  
on the mutual impedance

## CHAPTER 7

### CONCLUSIONS

This thesis has presented a combination of experimental and analytical procedures for computing the ground impedance of a power substation by the use of low current techniques. This is supported by the following results:

1) In Chapter 5 it was concluded that the 50 Hz ground impedance with a low current injection method is:

$$Z_g = 132 \angle 17 (1+3.5\%) \text{ m}\Omega$$

On the other hand, the result from the high current injection method is:

$$Z_g = 124 \angle 15 \text{ m}\Omega$$

A difference of only 5% is observed if we take the high current value as reference.

From the comparison of the measuring techniques, it is concluded that low current injection techniques give results comparable with a high current injection test, making them a practical choice for reasons of economy and safety.

2) Some authors have suggested measurement techniques using current injection at frequencies slightly different from 60 Hz. Just for comparison purposes, and since in this case the application of the frequency-scanning method permitted the evaluation of ground impedance values at 70 Hz, a similar analysis to the one presented in Chapter 5 arrived at the following results:

Average of  $Z_g$  at 70 Hz:  $139 \frac{19}{19}$  (m $\Omega$ )

Standard deviation s: 5.2 (m $\Omega$ )

Coefficient of variation v: 4.5%

For this particular site, the 70 Hz ground impedance was only 5% greater than the 60 Hz value. This is expected because the angle of 15 degrees in the final ground impedance indicates a strong resistive component. Nevertheless, it has to be emphasized that this is not a general conclusion for every case.

3) The field measurements reported in this thesis have shown that low current testing gives similar values at different angles between current and potential auxiliary leads, whenever the mutual coupling effects between them can be accounted for with the appropriate analytical tools. This is important since the choice of directions for the P and C leads is many times limited by field conditions.

4) Equations are developed to correct for the undesirable mutual effects between auxiliary leads, when one of the conductors is above the surface of the earth. When this height is set to zero, the expressions first reported in [46], are obtained. Hence, the equations reported here are applicable in a broader number of practical cases, mainly in measurements at urban and suburban areas. A sensitivity analysis unveils that height has almost no impact on the mutual impedance, and that the overhead conductor can be placed at any angle with respect to the one on the surface. With minor modifications, this work can be extended to the field of high frequencies.



## REFERENCES

1. Alderton, J.R., P.C. Anderson and R.J. Cakebread,  
"Calculation and Measurement of the Earth Impedance of  
an EHV. Substation", Proceedings IEE, vol. 125, No.  
12; December, 1978.
2. Bohn, R. Introduction to Electromagnetic Fields  
and Waves, (Massachusetts: Addison Wesley Publishing  
Co.) 1968.
3. Burington, R.S., Handbook of Mathematical Tables  
and Formulas (New York: McGraw-Hill Book Co.) 1973,  
p.86.
4. CSA STANDARD C22.1: Canadian Electrical Code, Part I,  
13th. Ed., Section 35-304 Station Ground Resistance.
5. Carson, J.R., "Wave Propagation in Overhead Wires with  
Ground Return", The Bell System Technical Journal,  
October 1926, pp.539-554.
6. Curdts, E.B., "Some of the Fundamental Aspects of Ground  
Resistance Measurements", AIEE Transactions, 1958,  
Vol.77, Part I, pp.760.
7. Dawalibi, F. and D. Mukhedkar, "Optimum Design of  
Substation Grounding in Two Layer Structure: Parts I,  
II, and III", IEEE Transactions on Power Apparatus  
and Systems, Vol. PAS-94, No. 2, March/April 1975,  
pp.252-272.

8. Dawalibi, F. and D. Mukhedkar, "Resistance Measurements of Large Grounding Systems", IEEE Transactions on Power Apparatus and Systems, Vol. PAS-98, 1979, pp. 2348-2354.
9. Dick, E.P., C.C. Erven and S.M. Harvey, "Grounding System Tests for Analysis of Fault-induced Voltages on Communication Cables", IEEE Transactions on Power Apparatus and Systems, Vol. PAS-98, 1979, pp. 2115-2125.
10. Dresden, A., Solid Analytical Geometry and Determinants (New York: John Wiley) 1930.
11. Duke, C.A., and L.E. Smith, "The Technique and Instrumentation of Low Impedance Ground Measurements", AIEE Transactions, Part I Vol. 77, November 1958, pp. 767-770.
12. EPRI: Transmission Line Grounding, Vol. 1, Report EL-2699 from project 1494-1 (October, 1982), Ch. 6
13. Feist, K.H., "Application of Current Injection Method for Checking the Earthing System of Substations", CIGRE-SC 23/W5 01, 1976.
14. Fortin, J., H.G. Sarmiento and D. Mukhedkar, "Experiences de Mesure dans le domaine des installations de Mise a la Terre", paper accepted for presentation at the CIGRE Symposium Courant de Fort Intensite dans les Reseaux, Brussels, Belgium, June 3-5, 1985.

15. Fortin, J., H.G. Sarmiento and D. Mukhedkar, "Field Measurement of Ground Fault Current Distribution and Substation Ground Impedance at LG-2, Quebec", paper 85 WM 117-7 presented at the IEEE PES Winter Meeting, New York, N.Y., February 3-8, 1985.

16. Fortin, J., H.G. Sarmiento, and D. Mukhedkar, "Determination of a Substation Ground Impedance with High Current Injection: Measurement and Analysis", Proceedings of the IEEE 1983 International Electrical and Electronics Conference, Vol. 2, pp. 34-37. (Toronto, Canada).

17. Foster, R.M., "Mutual Impedance of Grounded Wires Lying on the Surface of the Earth", The Bell System Technical Journal, Volume X, No. 3, July 1931, pp. 408-419.

18. Foster, R.M., "Mutual Impedance of Grounded Wires Lying on or Above the Surface of the Earth", The Bell System Technical Journal, July 1933, pp. 264-273.

19. Gagnon, J. and D. Mukhedkar, "Earth Resistivity Measurements in a Two Layer Earth Structure", paper C 74 195-2 presented at the IEEE PES Winter Meeting, New York, N.Y., Jan 27-Feb 1, 1974.

20. Hall, R., "Substation Ground Grid Resistance Measurements-Low Voltage Testing Techniques", paper A 75 460-6 presented at the IEEE PES Summer Meeting, Portland, Ore. July 18-23, 1976.

21. Harrison, L.H., "The Effect of Reactive Components in the Measurement of Grounding Circuits", AIEE Transactions, Vol. 72, Part II, 1953, pp.340-345.
22. Heppe, R.H., "Computation of Potential at Surface, Above an Energized Grid or Other Electrode, Allowing for Non-uniform Current Distribution", IEEE Transactions on Power Apparatus and Systems, Vol. Pas-98, No.6, pp.1978-1989, Nov/Dec 1979.
23. IEEE: Guide for Safety in Substation Grounding. IEEE Std. 80-1976.
24. IEEE. Guide for Measuring Earth Resistivity, Ground Impedance and Earth Surface Potentials of a Ground System, IEEE Std. 81-1983 (Revision of IEEE Std. 81-1962).
25. International Mathematical and Statistical Libraries Inc. Chapter I, Vol.2, June 1982.
26. Ironside, D.S., "Some Recent Developments in Portable Ground Resistance Test Instruments", EPRI Workshop on High Voltage Power System Grounding, May 12-14, 1982, Atlanta, Ga.
27. Kosztaluk, R., D. Mukhedkar and Y. Gervais, "Field Measurement of Touch and Step Voltages", IEEE Transactions on Power Apparatus and Systems, Vol. PAS-103, No. 11, November 1984, pp. 3286-3294.
28. Kuussaari, M. and A.J. Pesonen, "Earthing Impedance Measurements of Substations", CIGRE paper 36-02, 1978.

29. Laidig, J.F., and F.P. Zupa, "A Practical Ground Potential Rise Prediction Technique", IEEE Transactions on Power Apparatus and Systems, Vol. PAS-99, 1980, pp. 207-215.
30. Laws, Frank, A. Electrical Measurements (New York: McGraw-Hill Book Co.) 1938
31. Loeloeian, M., R. Velazquez, D. Mukhedkar and Y. Gervais, "Comparative Study of Different Methods for Calculating the Performance of Grounding Grids", Canadian Electrical Engineering Journal, Vol. 9, NO. 3, 1984, pp. 117-122.
32. Lu, I.D., and R.M. Shier, "Application of a Digital Signal Analyzer to the Measurement of Power System Ground Impedances", IEEE Transactions on Power Apparatus and Systems, April 1981, pp. 1919-1922.
33. Pesonen, A.J., "Effects of Shield Wires on the Potential Rise of HV Stations", SAHKO Electricity in Finland 53 (1980), No. 10, pp. 305-308.
34. Reynolds, P.H., D.S. Ironside, A.H. Silcocks and J.B. Williams, "A new Instrument for Measuring Ground Impedances", paper A 79 080-3 presented at the IEEE PES Winter Meeting, New York, N.Y., 1979.
35. Sarmiento, H.G., R. Valdivia and D. Mukhedkar, "Field Measurements of Power System Grounding Parameters in Energized Installations", IEEE Canadian Communications and Energy Conference Record, Montreal, Can. October 13-15, 1982, p. 161.

36. Sarmiento, H.G., R. Velazquez, J. Fortin and D. Mukhedkar, "Exact Ground Resistance (Impedance) Measurements", Electrical Safety'82, National Scientific Technical Conference, Sofia, Bulgaria, May 1-5, 1982.
37. Sarmiento, H.G., R. Velazquez, D. Mukhedkar, and R. Gilbert, "Reevaluation of Lethal Currents in the Human Body", Electrical Safety'82, National Scientific Technical Conference, Sofia, Bulgaria, May 1-5, 1982
38. Sarmiento, H.G., R. Valdivia and D. Mukhedkar, "Análisis de Sensitividad en el Diseño de la Red de Tierras de una Planta Termoelectrica", IEEE Mexican'80, Sección Mexico, Mexico City, October 22-25, 1980.
39. Sarmiento, H.G., J. Fortin and D. Mukhedkar, "Experienced-based Measurement of Grounding Parameters in Electrical Installations", Conference Record IEEE Industry Applications Society Annual Meeting, Mexico City, Mexico, October 3-7, 1983, pp. 425-430.
40. Sarmiento, H.G., J. Fortin, D. Mukhedkar, "Substation Ground Impedance: Comparative Field Measurements with High and Low Current Injection Methods", IEEE Transactions on Power Apparatus and Systems, Vol. PAS-103, No. 7, July 1984, pp. 1677-1683.

41. Sarmiento, H.G., R. Velazquez, J. Fortin, D. Mukhedkar,  
"Survey of Low Ground Electrode Impedance  
Measurements", IEEE Transactions on Power Apparatus  
and Systems, September, 1983, Vol. PAS-102, No. 9,  
pp. 2842-2849.
42. Seljeseth, H., A. Campling, K.H. Feist and  
M. Kuussaari, "Station Earthing-Safety and Interference  
Aspects", ELECTRA, Vol. 71 1980, pp. 47-59.
43. Sunde, E.D. Earth Conduction Effects in Transmission  
Systems, (New York: Dover Publications, Inc.) 1968.
44. Tagg, G.F., "Measurement of the Resistance of Physically  
Large Electrode Systems", Proceedings IEE, Vol. 117,  
No. 11, Nov. 1970, pp. 2185-2190.
45. Tagg, G.F. Earth Resistances (London: Newnes Ltd.)  
1964.
46. Velazquez, R., P.H. Reynolds and D. Mukhedkar, "Earth-Return  
Mutual Coupling Effects in Ground Resistance  
Measurements of Extended Grids", IEEE Transactions on  
Power Apparatus and Systems, June 1983, Vol. PAS-102,  
No. 6, pp. 1850-1857.
47. Velazquez, R., Contribution a L'etude des Electrode  
de Mise a la Terre, Ph.D. Thesis, Ecole Polytechnique  
de Montreal, September, 1983.
48. Wenner, F. "A Method of Measuring Resistivity", National  
Bureau of Standards, Scientific Paper 12, No. S-258,  
1916, p. 499

## APPENDIX A

### INSTRUMENTATION REQUIRED FOR MEASURING GROUND IMPEDANCE

#### A1) Introduction.

When the grounding system impedance of a particular substation is less than one ohm, the choice of proper instrumentation is of utmost importance to achieve a better signal-to-noise ratio in the presence of ambient noise, for any of the measuring techniques described in chapters three and four.

The following list, although not intended to be quantitatively and qualitatively complete, serves as a first analysis for choosing the required equipment.

#### A2) Instrumentation for Current Injection.

##### 1) Transformer

Purpose: To use as an ac current source of 50-100 A at power-frequency in the high current injection methods.

A single phase transformer with polarity reversal and secondary tapings is enough. A transformer with magnitude and phase control is used in the interference compensation method.



## 2) Mobile ac Generator

Purpose: To use as an ac current source of 50-100 A at a frequency different from 50 Hz in the high current injection methods.

Of course, if necessary, it could also be used to deliver power-frequency current.

## 3) Oscillator (Function Generator)

Purpose: For use as a sine wave current source at frequencies different from 50 Hz in the low current injection methods.

A capacity of 0.1-0.3 kVA is enough, but can be used together with a power amplifier to give the desired current magnitude. A phase-locked detector slaved to the oscillator is desirable, in order to keep the voltmeter tuned to the oscillator.

## 4) Power Amplifier.

Purpose: Increase the current magnitude in the injection circuit.

In the oscillator-voltmeter and frequency-scanning methods the injected current should be enough to produce a significant voltage change in the ground system under test,

with additional possibility for testing at different levels of current. A single phase unit with a capacity in the order of 0.30 kVA is recommended (of course, if the impedance of the injection circuit is high, more power will be needed to drive the necessary current).

#### 5) Noise Generator.

Purpose: Provide current and voltage signals over a wide frequency range, approximating white noise over the analysis band, in the frequency-scanning method.

Some spectrum analyzers have a built-in noise generator that could be conveniently used.

#### A3) Instrumentation for Current Measurement.

##### 1) Spectrum Analyzer

Purpose: In the frequency-scanning method, after the current and voltage signals are detected, the instrument is used to produce a frequency domain impedance plot. It is also used as a white noise generator in the frequency range desired.

It is necessary for the instrument to be dual channel in order to display the ratio and phase angle difference between the voltage and current signals at both input channels. A conventional network analyzer can be used, which digitizes and correlates the current transducer and

potential signals, switching the two channels alternatively over the integration (sampling) time. Nevertheless, frequency domain measurements are made faster if the instrument uses a Fast Fourier Transform (FFT) algorithm, where the two channels are simultaneously digitized, eliminating errors caused by temporary changes in test signal levels. Another useful characteristic is the measurement of the coherence function. This is a frequency domain measure of the fraction of the power output caused by the input. If this fraction is 1.0, the output at that frequency is caused entirely by the input, and the transfer function (impedance) is valid. If close to 0.0, the output is caused by something (noise) other than the measured input.

## 2) Analog or Digital Multimeters.

Purpose: Useful for monitoring currents and voltages during measurements, and continuity checks for current and potential probes.

When monitoring voltages, a high input impedance ( $1\text{ M}\Omega$ ) and a low millivolt range are required.

## 3) Transducers for Current Signals.

Purpose: Convert parameters to a suitable form for measurement.

#### 4) Transformer.

Purpose: When using the transmission line for current injection, it may be used to match the load impedance (mainly the transmission line reactance).

#### 5) Current Transformers.

Purpose: Measure test current in high current injection methods. Current transformers already installed can be conveniently used. For current measurements in other grounding elements (counterpoises, ground wires, etc.), split-core current transformers are normally used.

#### A4) Instrumentation for Potential Measurement.

1) Spectrum Analyzer (Already described above).

2) Analog or Digital Multimeters (Already described above).

3) Filters (for use with non-50 Hz methods).

Purpose: When a high ambient 60 Hz noise is detected on the potential probe, a 60 Hz rejection filter may be used. In the frequency-scanning method, a noise conditioning filter is used for protection from the effects of low frequency saturation.

4) Frequency Selective Voltmeter.

Purpose: To measure the voltage on the potential probe

resulting from the injected current at different frequencies. Power frequencies 5-10 Hz from the test frequency can be rejected by commercially available instruments.

A high input impedance is required (more than 100 k $\Omega$ ). Other useful characteristics are: resolution and bandwidth in the order of 0.1 Hz and 1 Hz respectively. A selectivity from mV to tens of volts is generally enough.

#### A5) General.

##### 1) Oscilloscope.

Purpose: Check waveforms and presence of signals in the current and potential probes.

##### 2) Light Beam Oscillographic Recorder.

Purpose: All voltage and current signals can be conveniently displayed on a strip of light sensitive paper, with the advantage that phase angles can be determined. (With a frequency response in the order of 5 kHz).

Measurement of the grounding system impedance components requires the recording of voltage and current amplitude and duration long enough so that magnitudes and phase angle differences can be accurately scaled from the oscillogram. Peak to peak amplitudes of 4 to 6.5 cm and

recording speeds of between 3 to 4 m/s will satisfy these requirements. Owing to an adjustable chart speed, it is possible to improve the accuracy of measurements for several phase angle displacements. It allows for some signal processing after the test: for example, disregarding noise, harmonics or assymetry. Newer models of oscillographic recorders are equipped with variable gain inputs, which allows for a simple calibration process of the signals to be measured.

### 3) Time Controller

Purpose: Test measurements can be controlled and synchronized from a central location; it is used to start the oscillograph, open and close one or two circuit breakers, and stop the oscillographic recorder. The sequence and duration of the various control signals can be adjusted.

### 4) Test Bench.

Purpose: Concentration of all signals for easy testing and reading. A typical test bench consists of the following items:

a) Supply Circuits (to satisfy the needs of the various pieces of equipment).

The supply source must be independent from power sources used in the high current power-frequency methods.

b) Isolating Transformers.

c) Calibration Circuits.

d) Oscillographic recorder.

e) Time controller.

**APPENDIX B**  
**THEORY OF THE FALL OF POTENTIAL METHOD**

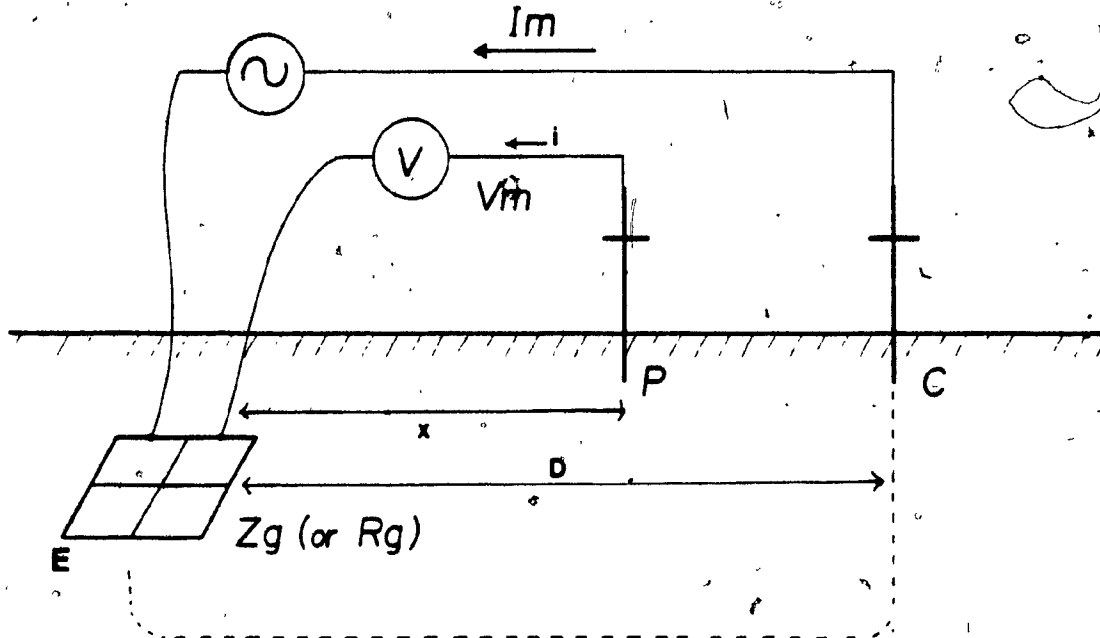


Figure B.1  
 Fall-of-Potential Method

**B1) Basic Definitions.**

- 1) If electrode E does not conduct any current into the soil, and is located faraway from any other current carrying electrodes, its self potential  $P_{ee}$  (or GPR) is zero.
- 2) If current  $I_m$  enters the soil through electrode E, its potential rises to  $P_{ee} = R_g(I_m)$ , where  $R_g$  is the electrode resistance (or impedance). If  $I_m = 1A$ , then:

$$P_{ee} = V_{ee} = R_g \times 1.0 = R_g$$



Therefore, in the following analysis,  $V_{ee}$  designates the potential rise of electrode E when 1A enters the soil through the electrode.  $V_{ee}$  is numerically equal to the electrode's resistance in ohms.

3) Assume that at some finite distance from electrode E, a current  $I_m$  is injected through the auxiliary current probe C. Because of the local earth potential rise, electrode E, initially at zero potential, will be at potential  $P_{ec}$  (this phenomena is often called "resistive coupling"). If  $I_m=1A$ , then  $P_{ec}=V_{ec}$  (numerically equal to the so called "mutual resistance" between E and C).

4) If electrode E carries 1A while simultaneously electrode C conducts 1A as well, the potential rise of electrode E will be  $V_{ee} + V_{ec}$ .

## B2) Fundamental Equations.

Current "i" in electrode P is assumed negligible with respect to  $I_m$ . At a given time "t", current  $I_m$  injected into the ground through E is assumed positive, and  $I_m$  collected by C, is assumed negative.

If  $U_p$  and  $U_e$  represent the GPR (with respect to remote ground) of electrodes P and E respectively, then based on the definitions previously presented:

$$U_p = V_{pe} \times I'_m + V_{pc} \times (-I'_m) \quad (B.1)$$

$$U_e = V_{ee} \times I'_m + V_{ec} \times (-I'_m) \quad (B.2)$$

where:

$$I'_m = I_m / 1.0 \text{ A}$$

The voltage  $V_m$  measured by the fall of potential method is:

$$V_m = U_e - U_p$$

$$V_m = I'_m (V_{ee} - V_{ec} - V_{pe} + V_{pc}) \quad (B.3)$$

As seen before,  $V_{ee}$  is the potential rise of electrode E resulting from its own current of 1A. This is by definition the resistance  $R_g$  of electrode E.

Therefore, eq. (B.3) becomes:

$$R_m = \frac{V_m}{I_m} = R_g + (V_{pc} - V_{ec} - V_{pe}) / 1A \quad (B.4)$$

$V_{pc}$  and  $V_{pe}$  are functions of the spacing between the electrodes (E, C, P), the electrode configuration, and the soil characteristics.

According to figure B.1, let us define the functions  $f$ ,  $g$ ,  $h$  assuming they are only functions of distances  $D$  and  $x$ :

$$V_{ec} = f(D)$$

$$V_{pc} = g(D-x)$$

$$V_{pe} = h(x)$$

According to eq. (B.4), the measured resistance will be equal to the true resistance  $R_g$  if:

$$V_{pc} - V_{ec} - V_{pe} = 0$$

or

$$g(D-x) - f(D) - h(x) = 0 \quad (B.5)$$

### B3) Identical Electrodes and Large Spacings.

If electrodes E and C are identical  $g=h$ , and if D is large enough such that  $V_{ec} = f(D) = 0$ , then condition (B.5) becomes:

$$g(D-x) - h(x) = 0$$

thus

$$x_0 = D/2$$

which means, the auxiliary potential probe should be located midway between E and C.

### B4) Hemispherical Electrodes.

If electrodes E and C are hemispheres and their radii are small compared to  $x$  and  $D$  and if soil is uniform, then

the potential functions  $f$ ,  $g$ , and  $h$  are inversely proportional to the distance relative to the hemisphere center. If the origin of the axes is at the center of hemisphere E, the eq. (B.5) becomes:

$$1/(D-x) - 1/D - 1/x = 0 \quad (B.6)$$

The positive root of eq. (B.6) is the exact potential probe location  $x_0$ :

$$x_0 = 0.518D$$

This is the well known 61.8% rule [6].

#### B5) General Case.

If the soil is not homogeneous, or electrodes E and C have complex configurations, or both; the functions  $f$ ,  $g$ , and  $h$  are not easy to calculate. In such cases, computer solutions are generally required. [7,8].

## APPENDIX C

### SCREENING FACTOR AT YAMASKA SUBSTATION

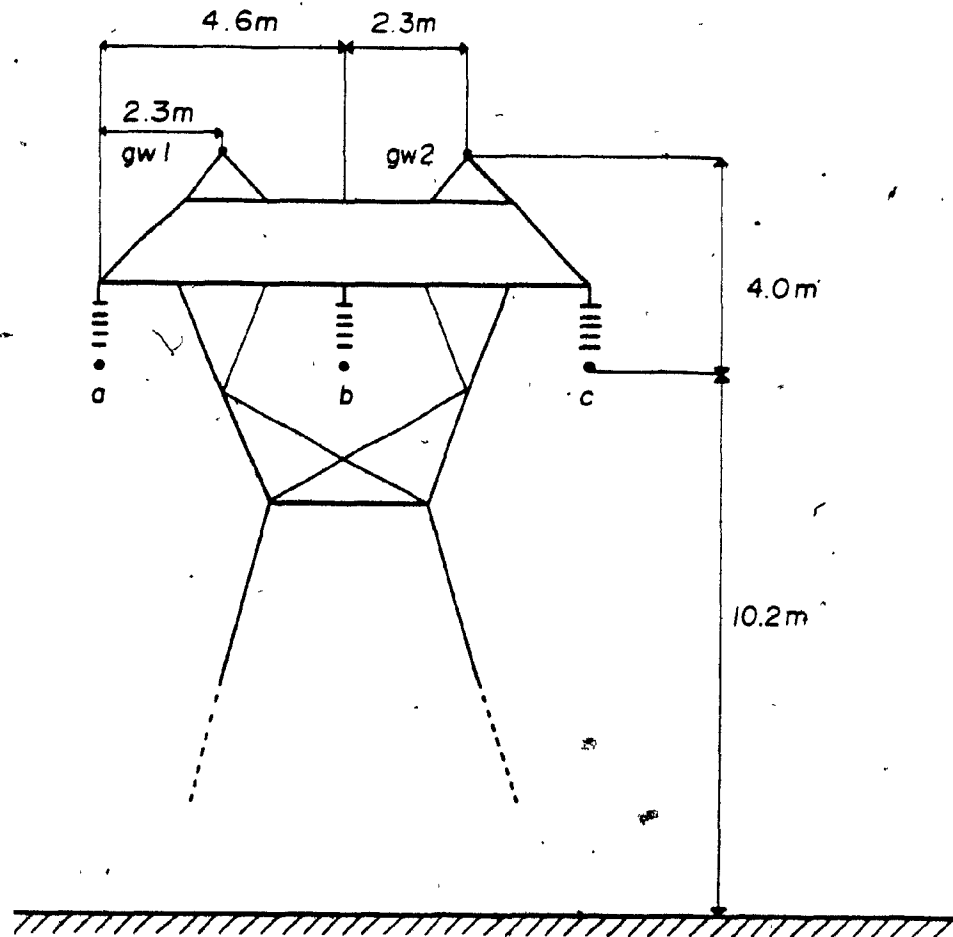


Figure C.1

Single Circuit, 120 kV line at Yamaska Substation.

To Calculate the screening factor described in Chapter 3, we need the following distances: (Refer to Figure C.1)

$$Da(gw1) = \sqrt{4^2 + 2.3^2} = 4.51 \text{ m}$$

$$D_c(gw2) = 4.51 \text{ m}$$

$$D_a(gw2) = \sqrt{6.9^2 + 4.0^2} = 7.97 \text{ m}$$

$$D_c(gw1) = 7.97$$

$$D_b(gw1) = D_b(gw2) = 4.51 \text{ m}$$

$$D(gw1)(gw2) = 4.5 \text{ m}$$

The characteristics of the two ground wires are as follows:

$$\text{Resistance} = 4.2 \text{ ohm/km}$$

$$\text{GMR (Geometric Mean Radius)} = 2.4 \times 10^{-8} \text{ m}$$

Figure C.2 displays the output from the computer program:

RESISTIVITY OF THE SOIL IN OHM-M.: 28.10  
FREQUENCY IN HERTZ: 60.00  
NUMBER OF GROUND WIRES: 2.

---

RESISTANCE OF GROUND RETURN EFFECT(OHM/MI.): 0.28584  
REACTANCE OF GROUND RETURN EFFECT(OHM/MI.): 2.65639

---

RESISTANCE OF THE GROUND WIRE(OHM/MI.): 6.760  
REACTANCE OF THE GROUND WIRE(OHM/MI.): 1.984

---

DISTANCES BETWEEN PHASES AND GROUND WIRES:  
15.10 15.10 15.10 15.10 26.20 26.20  
DISTANCE(IN F.T.) BETWEEN THE TWO GROUND WIRES:  
15.10

---

MAGNITUDE OF SELF IMPEDANCE= 11.62359 ANGLE= 26.24  
MAGNITUDE OF MUTUAL IMPEDANCE= 1.62680 ANGLE= 79.88  
MAGNITUDE OF ZMUTUAL/ZSELF= 0.13996 ANGLE=53.64

---

MAGNITUDE OF 1.-ZMUT/ZSELF= 0.92393 ANGLE= -7.01

---

FIGURE C.2

Output from computer program

Consequently, the screening factor used for calculating the final ground impedance at Yamaska is:

$$r = 0.92393 \angle -7$$

[illegible]

(Printed with permission from Hydro-Quebec).

- 129 -



taken by shortcircuiting to earth the secondary of the transformer, all signals must be calibrated. In short, this means knowing in advance how many volts/cm corresponds to each output channel in the oscillographic recorder.

After the calibration is finished, all signals are identified, and once the actual measurements are made; it is only required to measure the distance in cm between peak to peak in all voltage or current sinusoidal waves. Although not quite apparent from figure D.1, all measurements should be made after the dc offset disappears.

For the grounding tests at Yamaska, five short circuit tests were done, with the three phases of the transmission line connected together. The oscillographic recorder yielded the following magnitudes of fault current:

s.c. no. 1	586.14 A
s.c. no. 2	594.51 A
s.c. no. 3	595.08 A
s.c. no. 4	595.91 A
s.c. no. 5	583.23 A

The average of the five current magnitudes, and the value used in further calculations is:

$$I_m = 591 \text{ A}$$

In each of the five short circuits, potential rise

measurements were procured at the three potential probe locations shown in table 5.1. These potential readings were then scaled to the average fault current, giving the following results:

P = 1310 m       $V_m = 66.54$  V

P = 1490 m       $V_m = 68.09$  V

P = 1830 m       $V_m = 68.13$  V

Finally, the three ground impedance values appearing in Table 5.1 resulted from the ratio  $V_m/I_m$ .